UNIVERSIDAD DE CONCEPCIÓN

Centro de Investigación en Ingeniería Matemática (CI^{2}MA)

CI^{2}MA

Centro de Investigación en Ingeniería Matemática

A coupled HDG discretization for the interaction between acoustic and elastic waves

Fernando Artaza-Covarrubias, Tonatiuh Sanchez-Vizuet, Manuel Solano

PREPRINT 2025-22

SERIE DE PRE-PUBLICACIONES

A coupled HDG discretization for the interaction between acoustic and elastic waves

Fernando Artaza-Covarrubias*[1], Tonatiuh Sánchez-Vizuet†[2], and Manuel Solano‡[1,3]

[1]Department of Applied Mathematics, University of Waterloo, Ontario, Canada.
[3]Departamento de Ingeniería Matemática, Facultad de Ciencias Físicas y Matemáticas, Universidad de Concepción, Concepción, Chile.
[3]Center for Research in Mathematical Engineering CI²MA, Universidad de Concepción, Concepción, Chile.
[2]Department of Mathematics, The University of Arizona, USA.

September 29, 2025

Abstract

We propose and analyze an HDG scheme for the Laplace-domain interaction between a transient acoustic wave and a bounded elastic solid embedded in an unbounded fluid medium. Two mixed variables (the stress tensor and the velocity of the acoustic wave) are included while the symmetry of the stress tensor is imposed weakly by considering the antisymmetric part of the strain tensor (the spin or vorticity tensor) as an additional unknown. Convergence of the method is demonstrated and theoretical rates are obtained; numerical results suggesting optimal order of convergence and superconvergence of the traces are presented.

Keywords: Acoustic waves elastic waves; Hybridizable Discontinuous Galerkin; Coupled HDG; wave-structure interaction.

Mathematics Subject Classification (2020) 74J05, 65M60, 65M15, 65M12.

1 Introduction

We are interested in the computational simulation of the interaction between a transient acoustic wave and a homogeneous, isotropic and linearly elastic solid. The physical setting of the problem is as follows. An incident acoustic wave, represented by its scalar velocity potential v^{inc}, propagates at constant speed c in a homogeneous, isotropic and irrotational fluid with density ρ_f filling a region Ω_A and impinges upon an elastic body of density ρ_E contained in a bounded region Ω_E with Lipschitz boundary Γ and exterior unit normal vector $\boldsymbol{n}_E$. Part of the energy and momentum carried by the acoustic wave is transferred to the elastic solid, exciting an internal elastic wave $\boldsymbol{u}$, while the remaining momentum and energy are carried by an acoustic wave v that is scattered off the surface Γ of the elastic body. The physical setting is represented graphically in the left panel of Figure 1.

Due to the linearity of the problem, the total acoustic wave $v^{\text{tot}} = v^{\text{inc}} + v$ is the superposition of the known incident field v^{inc} and the unknown scattered field v. The unknowns are thus the scattered acoustic field v and the excited elastic displacement field $\boldsymbol{u}$ that satisfy the following system of time-dependent partial differential equations [50]:

$$
\begin{aligned}
-\nabla\cdot\left(2\mu\boldsymbol{\varepsilon}\left(\boldsymbol{u}\right)+\lambda\nabla\cdot\boldsymbol{u}\boldsymbol{I}\right)+\rho_E\ddot{\boldsymbol{u}} &= \boldsymbol{f} && \text{in } \Omega_E,\\
-\Delta v + c^{-2}\ddot{v} &= f && \text{in } \Omega_A,\\
\nabla v^{\text{tot}}\cdot\boldsymbol{n}_E + \dot{\boldsymbol{u}}\cdot\boldsymbol{n}_E &= 0 && \text{on } \Gamma,\\
\rho_f\dot{v}^{\text{tot}}\boldsymbol{n}_E + \left(2\mu\boldsymbol{\varepsilon}\left(\boldsymbol{u}\right)+\lambda\nabla\cdot\boldsymbol{u}\boldsymbol{I}\right)\boldsymbol{n}_E &= \boldsymbol{0} && \text{on } \Gamma,
\end{aligned}
$$

*fartaza2019@udec.cl
†tonatiuh@arizona.edu
‡msolano@ing-mat.udec.cl

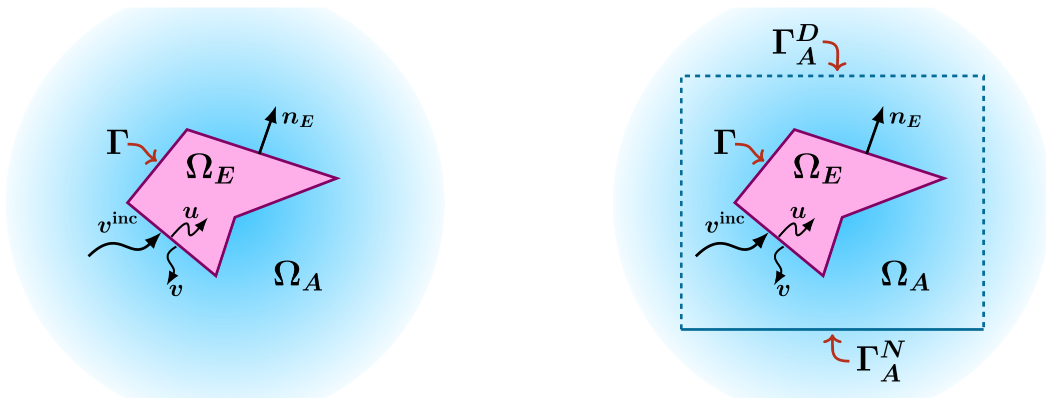

Figure 1: Schematic representation of the problem geometry. Left: The elastic domain Ω_E is bounded; its Lipschitz boundary is denoted as Γ. The domain Ω_A where the acoustic waves propagate is unbounded. Right: An artificial boundary Γ_A enclosing the elastic domain is introduced. The artificial boundary is split onto two disjoint components Γ_A^D and Γ_A^N where Dirichlet and Neumann boundary conditions are imposed respectively.

including suitable initial and radiation conditions, where the upper dot represents differentiation with respect to time, $\boldsymbol{\varepsilon}(\boldsymbol{u}) := \frac{1}{2}(\nabla \boldsymbol{u} + \nabla^\top \boldsymbol{u})$ is the strain tensor, $\boldsymbol{I}$ is the identity tensor, $\boldsymbol{f}$ and f are square integrable source terms for every time, and the Lamé constants, μ (shear modulus) and λ (Lamé's first parameter), encode the material properties of the solid. The symmetric tensor

$$\boldsymbol{\sigma} := 2\mu\boldsymbol{\varepsilon}(\boldsymbol{u}) + \lambda \nabla\cdot \boldsymbol{u}\boldsymbol{I}$$

is known as the Cauchy stress tensor and can be represented compactly as $\boldsymbol{\sigma} = \mathbf{C}\boldsymbol{\varepsilon}(\boldsymbol{u})$, where Hooke's elasticity tensor $\mathbf{C}$ is defined by its action on an arbitrary square matrix $\boldsymbol{M}$ as

$$\mathbf{C}\boldsymbol{M} := 2\mu\boldsymbol{M} + \lambda \mathrm{tr}(\boldsymbol{M})\boldsymbol{I} \quad \text{and} \quad \mathbf{C}^{-1}(\boldsymbol{M}) := \frac{1}{2\mu}\boldsymbol{M} - \frac{\lambda}{2\mu(n\lambda + 2\mu)}\mathrm{tr}(\boldsymbol{M})\boldsymbol{I},$$

where $\mathrm{tr}(\boldsymbol{M}) := \sum_{i=1}^{n} M_{ii}$ is the matrix trace operator. We will follow the approach from [20], where the symmetry of the stress tensor $\boldsymbol{\sigma}$ is imposed weakly by introducing the spin (or vorticity) tensor

$$\boldsymbol{\gamma}(\boldsymbol{u}) := (\nabla \boldsymbol{u} - \nabla^\top \boldsymbol{u})/2$$

as an additional unknown.

When viewed in full generality, the acoustic propagation region Ω_A is in fact unbounded and given by $\Omega_A := \mathbb{R}^n \setminus \overline{\Omega_E}$. This fact introduces further computational challenges that are often addressed either through an integral equation representation of the acoustic wave [4, 36, 37, 51], the introduction of a perfectly matched layer [39], the use of absorbing boundary conditions [24, 34, 35, 55] or the representation of the acoustic field through a moment expansion [1].

In this communication, we simplify the analysis by introducing an artificial boundary that will allow us to assume that the acoustic domain is in fact bounded. As depicted in the right panel of Figure 1, we pick a polygon with boundary Γ_A (the subscript standing for "artificial") that compactly contains the elastic domain Ω_E. The boundary Γ_A is divided into mutually disjoint Dirichlet and Neumann segments (denoted respectively by Γ_A^D and Γ_A^N) such that $\Gamma_A = \Gamma_A^D \cup \Gamma_A^N$. The acoustic domain Ω_A is then defined to be the region exterior to Ω_E and contained inside the polygon. Its boundary takes the form

$$\partial\Omega_A := \Gamma \cup \Gamma_A^D \cup \Gamma_A^N$$

where the three components are mutually disjoint and Γ denotes the interface between the acoustic and elastic regions. We emphasize that the boundary conditions imposed on Γ_A do not attempt to account for a physically outgoing wave, but simply to ensure the well-posedness of the simplified problem. The goal of this work is to establish the well-posedness theory for the coupling of HDG discretizations for elastic and acoustic wave propagation. The treatment of the fully unbounded problem with appropriate outgoing boundary conditions will be the subject of a separate communication.

Assuming that at the initial time the incident wave v^{inc} is supported away from the elastic domain Ω_E, the distributional version of the system above admits a Laplace transform [37] that maps time differentiation to multiplication by the Laplace parameter $s \in \{z \in \mathbb{C} : \text{Re}(z) > 0\}$. Upon Laplace transformation and using the same symbols for the unknowns in the time domain and in the Laplace domain, the elastic wave $\boldsymbol{u}$ and the scattered acoustic wave v satisfy the coupled system of equations in mixed form

$$\mathbf{C}^{-1}\boldsymbol{\sigma} - \nabla \boldsymbol{u} + \boldsymbol{\gamma} = \mathbf{0} \qquad \text{in } \Omega_E, \tag{1a}$$

$$-\nabla\cdot \boldsymbol{\sigma} + \rho_E s^2 \boldsymbol{u} = \boldsymbol{f} \qquad \text{in } \Omega_E, \tag{1b}$$

$$\boldsymbol{q} - \nabla v = \mathbf{0} \qquad \text{in } \Omega_A, \tag{1c}$$

$$-\nabla\cdot \boldsymbol{q} + (s/c)^2 v = f \qquad \text{in } \Omega_A, \tag{1d}$$

$$\boldsymbol{q}\cdot\boldsymbol{n}_A - s\,\boldsymbol{u}\cdot\boldsymbol{n}_E = -\nabla v^{\text{inc}}\cdot\boldsymbol{n}_A \qquad \text{on } \Gamma, \tag{1e}$$

$$-\boldsymbol{\sigma}\boldsymbol{n}_E + \rho_f\, s\, v\, \boldsymbol{n}_A = -\rho_f\, s\, v^{\text{inc}}\, \boldsymbol{n}_A \qquad \text{on } \Gamma, \tag{1f}$$

$$v = g_D \qquad \text{on } \Gamma_A^D, \tag{1g}$$

$$\boldsymbol{q}\cdot\boldsymbol{n}_A = g_N \qquad \text{on } \Gamma_A^N. \tag{1h}$$

Here, $\boldsymbol{q}$ is the acoustic velocity field, and $g_D \in H^{1/2}(\Gamma_A^D)$ and $g_N \in H^{-1/2}(\Gamma_A^N)$ are given boundary data.

In the system above, equations (1a) and (1b) account for the Navier-Lamé or elastic wave equation in the interior of the elastic solid Ω_E. Similarly, equations (1c) and (1d) are the mixed form of the acoustic wave equation in Ω_A. The elastic and acoustic variables are coupled through the continuity of the normal component of the velocity field across the interface Γ, encoded in equation (1e), and the balance of normal forces at the contact surface, given in (1f). The nonphysical boundary conditions (1g) and (1h) prescribed at the artificial boundary Γ_A are given to ensure the well-posedness of the problem.

In the literature, there is a vast amount of research related to fluid-structure interaction problems. For instance, some of them use a Mixed Finite Elements approach [23, 29] and there are also couplings of this technique with Boundary Element Methods [28]. Studies on their spectral problems [41] and an analysis of the elastoacustic problem in the time domain [2] have been done. However, most of these works assume a time-harmonic regime, while we intend to focus on the transient regime. A notable time–domain contribution is the very recent contribution [42], where a Hybrid High Order (HHO) method is used for a similar acoustic/elastic interaction in the time domain.

Since two different systems of PDEs posed in different domains are being coupled across an interface, we prefer to use a discontinuous Galerkin scheme due to its flexibility to handle the transmission conditions. In particular, by considering the HDG method introduced in [16], it is very easy to impose transmission conditions from the computational point of view. In fact, in HDG schemes the only globally coupled degrees of freedom are precisely those of the numerical traces on the boundaries between elements, while the remaining unknowns are obtained by solving local problems in each element. Therefore, if we have two independent HDG solvers, one for the acoustic problem and another one for the elastic system, we can couple them across the interface through the numerical traces associated with the acoustic wave v and the elastic displacements $\boldsymbol{u}$.

After [16] and the pioneering work [18] that set a framework that simplifies the analysis of a family of HDG schemes by introducing a suitable projection, HDG schemes have been developed for a wide variety of problems. For example, convection-diffusion equation [27, 43], Stokes flow [17, 30]; Brinkman, Oseen and Navier–Stokes equations [8, 9, 26, 45]. In the context of electromagnetism and wave propagation problems, HDG schemes have also been introduced: Maxwell's operator [11, 12], eddy current problems [5], Maxwell's equations in the frequency-domain [25, 44] and heterogeneous media [6] and Helmholtz equation [10, 32, 57], and even for nonlinear problems arising from plasma physics [47, 48, 52, 53]. For the elasticity problem, we refer the reader to [20, 46]. The preceding list of references is not exhaustive, but provides an overview of the development of HDG schemes during the last fifteen years.

On the other hand, in the context of coupled problems with piecewise linear interfaces, HDG schemes have been proposed for elliptic [38] and for the Stokes interface problems [56], and for Stokes-Darcy coupling [31]. The influence of hanging-nodes along the interface and the use of different polynomial degree over each local space, have been analyzed in [13, 14]. Recently, a new approach based on the Transfer Path Method [19, 21, 49] has been proposed to handle discrete interfaces that do not necessarily coincide with the true interface, as in the case of a curved interface [3, 40, 54]. This technique produces a high order method and is closely related with our ultimate goal, where it is crucial to have a numerical scheme that couples an HDG discretization of the problem posed in an bounded domain considering a solid with a curved boundary, and a representation of the acoustic wave in the unbounded region. To the best of our knowledge, the use of HDG schemes has not been analyzed for the coupled problem (1), and the main contribution of this work is to provide a convergence analysis.

2 Preliminaries and notation

2.1 Sobolev spaces.

Let $\mathcal{O}$ be a Lipschitz continuous domain in $\mathbb{R}^n$. We use standard notations for Lebesgue $\mathrm{L}^t(\mathcal{O})$ and Sobolev spaces $\mathrm{W}^{l,t}(\mathcal{O})$, with $l \geq 0$ and $t \in [1,+\infty)$. Here $\mathrm{W}^{0,t}(\mathcal{O}) = \mathrm{L}^t(\mathcal{O})$, and if $t = 2$ we write $\mathrm{H}^l(\mathcal{O})$ instead of $\mathrm{W}^{l,2}(\mathcal{O})$, with the corresponding norm and seminorm denoted by $\|\cdot\|_{H^l(\mathcal{O})}$ and $|\cdot|_{H^l(\mathcal{O})}$, respectively. The spaces of vector-valued functions will be denoted in boldface, therefore $\boldsymbol{H}^s(\mathcal{O}) := [H^s(\mathcal{O})]^n$, whereas for tensor-valued functions, we write $\underline{\boldsymbol{H}}^s(\mathcal{O}) := [H^s(\mathcal{O})]^{n\times n}$. Using the same notation, we write $\boldsymbol{L}^2(\mathcal{O}) := [L^2(\mathcal{O})]^n$ and $\underline{\boldsymbol{L}}^2(\mathcal{O}) := [L^2(\mathcal{O})]^{n\times n}$.

The complex L^2-inner products will be denoted by $(\cdot,\cdot)_{\mathcal{O}}$ and $\langle\cdot,\cdot\rangle_\Sigma$, where Σ is either a Lipschitz curve ($n = 2$) or a surface ($n = 3$). The associated norms will be denoted by $\|\cdot\|_{\mathcal{O}}$ and $\|\cdot\|_\Sigma$.

It is easy to verify that Hooke's tensor satisfies the following inequalities for all $\boldsymbol{\eta} \in \underline{\boldsymbol{L}}^2(\mathcal{O})$:

$$\left(\frac{1}{2\mu} + \frac{n^2\lambda}{2\mu(n\lambda+2\mu)}\right)^{-1} \|\boldsymbol{\eta}\|^2_{\mathcal{O},\mathbf{C}^{-1}} \leq \|\boldsymbol{\eta}\|^2_{\mathcal{O}} \leq 2\mu\|\boldsymbol{\eta}\|^2_{\mathcal{O},\mathbf{C}^{-1}},$$

$$\|\boldsymbol{\eta}\|^2_{\mathcal{O},\mathbf{C}} \leq (2\mu + n^2\lambda)\|\boldsymbol{\eta}\|^2_{\mathcal{O}},$$

where we denote $\|\cdot\|_{\mathcal{O},\mathbf{C}^{-1}} := (\mathbf{C}^{-1}\cdot,\cdot)^{1/2}_{\mathcal{O}}$ and $\|\cdot\|_{\mathcal{O},\mathbf{C}} := (\mathbf{C}\cdot,\cdot)^{1/2}_{\mathcal{O}}$.

2.2 Mesh and mesh-dependent inner products.

Let $\mathcal{T}_A$ and $\mathcal{T}_E$ be two families of regular triangulations of Ω_A and Ω_E, respectively. We will assume that these triangulations are compatible along the common interface Γ and that both are characterized by a common mesh size h in their respective domains. Given an element K, h_K will denote its diameter and $\boldsymbol{n}_K$ its outward unit normal. When there is no confusion, we will simply write $\boldsymbol{n}$ instead of $\boldsymbol{n}_K$. Set $\dagger \in \{A, E\}$, then $\partial\mathcal{T}_\dagger := \{\partial K : K \in \mathcal{T}_\dagger\}$ and let $\mathcal{E}_\dagger$ denote the set of all faces F of all elements $K \in \mathcal{T}_\dagger$. We will also use the following notation for L^2 inner products of scalar-, vector- and tensor-valued functions, respectively, over an integration domain D:

$$(u,v)_D := \int_D u\overline{v}, \qquad (\boldsymbol{u},\boldsymbol{v})_D = \int_D \boldsymbol{u}\cdot\overline{\boldsymbol{v}}, \qquad (\boldsymbol{M},\boldsymbol{N})_D = \int_D \boldsymbol{M} : \overline{\boldsymbol{N}},$$

where the overline denotes complex conjugation and the colon ":" is used to denote the Frobenius inner product of matrices

$$\boldsymbol{M} : \boldsymbol{N} := \sum_{i,j=1}^n M_{ij}N_{ij}.$$

With this notation we can express the mesh-dependent L^2 inner products as

$$(u,v)_{\mathcal{T}_\dagger} := \sum_{K\in\mathcal{T}_\dagger} (u,v)_K\,, (\boldsymbol{u},\boldsymbol{v})_{\mathcal{T}_\dagger} := \sum_{K\in\mathcal{T}_\dagger} (\boldsymbol{u},\boldsymbol{v})_K\,, \quad (\boldsymbol{M},\boldsymbol{N})_{\mathcal{T}_\dagger} := \sum_{K\in\mathcal{T}_\dagger} (\boldsymbol{M},\boldsymbol{N})_K\,,$$

along with the inner products over the mesh skeleton

$$\langle u,v\rangle_{\partial\mathcal{T}_\dagger} := \sum_{K\in\mathcal{T}_\dagger} \langle u,v\rangle_{\partial K}\,, \langle \boldsymbol{u},\boldsymbol{v}\rangle_{\partial\mathcal{T}_\dagger} := \sum_{K\in\mathcal{T}_\dagger} \langle \boldsymbol{u},\boldsymbol{v}\rangle_{\partial K}\,, \langle \boldsymbol{M},\boldsymbol{N}\rangle_{\partial\mathcal{T}_\dagger} := \sum_{K\in\mathcal{T}_\dagger} \langle \boldsymbol{M},\boldsymbol{N}\rangle_{\partial K}\,.$$

We denote the norms induced by these inner products by

$$\|\cdot\|_{\mathcal{T}_\dagger} := \sqrt{(\cdot,\cdot)_{\mathcal{T}_\dagger}} \qquad \text{and} \qquad \|\cdot\|_{\partial\mathcal{T}_\dagger} := \sqrt{\langle\cdot,\cdot\rangle_{\partial\mathcal{T}_\dagger}}.$$

Finally, to avoid proliferation of superflous constants, we will write $a \lesssim b$ when there exists a positive constant C, independent of the mesh size, such that $a \leq Cb$.

2.3 The HDG polynomial spaces

We will make use of the discrete spaces for the HDG method proposed in [20] for simplices. For an element $K \in \mathcal{T}_A \cup \mathcal{T}_E$, we define the following function spaces. The set of scalar-valued polynomials of degree at most k defined over K will be denoted by $\mathcal{P}_k(K)$, while the corresponding vector and tensor product spaces are denoted respectively as

$$\boldsymbol{\mathcal{P}}_k(K) := [\mathcal{P}_k(K)]^n \qquad \text{and} \qquad \underline{\boldsymbol{\mathcal{P}}}_k(K) := [\mathcal{P}_k(K)]^{n\times n}.$$

The polynomial spaces of degree *exactly* k will be denoted with a tilde as $\widetilde{\mathcal{P}}_k(K)$, $\widetilde{\boldsymbol{\mathcal{P}}}_k(K)$, and $\widetilde{\underline{\boldsymbol{\mathcal{P}}}}_k(K)$. We now define

$$A_{ij}\,(K) := \begin{cases} \mathcal{P}_k(K) & \text{if} \quad i \neq j, \\ 0 & \text{if} \quad i = j, \end{cases},$$

and use it to construct the matrix-valued space

$$\underline{\boldsymbol{A}}(K) := [A_{ij}\,(K)]^{n\times n}.$$

We will denote the space of L^2 integrable skew-symmetric matrices over K by

$$\underline{\boldsymbol{AS}}(K) := \{\boldsymbol{M} \in \underline{\boldsymbol{L}}^2(K) : \boldsymbol{M} + \boldsymbol{M}^\top = \boldsymbol{0}\},$$

and will require that $\underline{\boldsymbol{A}}(K) \subset \underline{\boldsymbol{AS}}(K)$.

Now, we would like to define a divergence-free space of functions through the use of bubble matrices or bubble scalars, depending on the dimension, as in [7, 15, 20, 33]. Following [33], a matrix-valued function $\boldsymbol{b}$ defined in Ω_E is said to be an admissible bubble matrix if for each $K \in \mathcal{T}_E$ the matrix $\boldsymbol{b}_K := \boldsymbol{b}|_K$ is a matrix with polynomial entries that satisfies

1. The tangential components of each row of $\boldsymbol{b}_K$ vanish on all the faces of K,
2. There exists $C_1 > 0$ such that $C_1(\boldsymbol{v}, \boldsymbol{v})_K \leq (\boldsymbol{v}\boldsymbol{b}_K, \boldsymbol{v})_K$, for all $\boldsymbol{v} \in \underline{\boldsymbol{L}}^2(K)$,
3. There exists $C_2 > 0$ such that $\|\boldsymbol{b}_K\|_{\underline{\boldsymbol{L}}^\infty(K)} \leq C_2$,

where the constants C_1 and C_2 depend only on the shape regularity of $\mathcal{T}_E$.

Thus, following [15, 20], if η_F is the barycentric coordinate associated to the edge F of K, and if we define

$$\boldsymbol{b}_K := \begin{cases} \displaystyle\prod_{F\subset\partial K} \eta_F & \text{in 2D}, \\ \displaystyle\sum_{F\subset\partial K} \left[\prod_{F'\subset\partial K\setminus\{F\}} \eta_{F'}\right] \nabla\eta_F \otimes \nabla\eta_F & \text{in 3D}, \end{cases}$$

the polynomial space $\underline{\boldsymbol{B}}(K)$ associated to bubble functions is defined as:

$$\underline{\boldsymbol{B}}(K) := \nabla \times ((\nabla \times \underline{\boldsymbol{A}}(K))\boldsymbol{b}_K).$$

We can observe that any function

$$\boldsymbol{v} \in \underline{\boldsymbol{\mathcal{B}}}_h := \{\boldsymbol{\eta} \in \underline{\boldsymbol{L}}^2(\Omega_E) : \boldsymbol{\eta}|_K \in \underline{\boldsymbol{B}}(K)\,, K \in \mathcal{T}_E\}$$

is such that

$$\nabla\cdot \boldsymbol{v}|_K = 0, \forall\, K \in \mathcal{T}_E \qquad \text{and} \qquad \boldsymbol{v}\boldsymbol{n}|_F = 0, \forall F \in \mathcal{E}_E.$$

In the three-dimensional case the curl operator acts row-wise, while in the two-dimensional case the curl of matrices and column vectors are defined respectively by

$$\nabla \times \begin{pmatrix} M_{11} & M_{12} \\ M_{21} & M_{22} \end{pmatrix} := \begin{pmatrix} \partial_x M_{12} - \partial_y M_{11} \\ \partial_x M_{22} - \partial_y M_{21} \end{pmatrix} \quad \text{and} \quad \nabla \times \begin{pmatrix} m_1 \\ m_2 \end{pmatrix} := \begin{pmatrix} -\partial_y m_1 & \partial_x m_1 \\ -\partial_y m_2 & \partial_x m_2 \end{pmatrix}$$

We will also make use of the local space $\underline{\boldsymbol{V}}(K) := \underline{\boldsymbol{\mathcal{P}}}_k(K) + \underline{\boldsymbol{B}}(K)$, and notice that

$$\underline{\boldsymbol{V}}(K) = \underline{\boldsymbol{\mathcal{P}}}_k(K) + \nabla \times ((\nabla \times \underline{\boldsymbol{A}}(K))\boldsymbol{b}_K) = \underline{\boldsymbol{\mathcal{P}}}_k(K) \oplus \nabla \times ((\nabla \times \widetilde{\underline{\boldsymbol{A}}}(K))\boldsymbol{b}_K),$$

where $\widetilde{\underline{\boldsymbol{A}}}(K) := \underline{\boldsymbol{A}}(K) \cap \widetilde{\underline{\boldsymbol{\mathcal{P}}}}_k(K)$.

3 An HDG discretization

Let us begin by introducing the piecewise polynomial spaces

$$\begin{aligned}
\underline{\boldsymbol{V}}_h &= \{\boldsymbol{\tau} \in \underline{\boldsymbol{L}}^2(\mathcal{T}_E) : \boldsymbol{\tau}|_K \in \underline{\boldsymbol{V}}(K)\,, \quad \forall K \in \mathcal{T}_E\}, && \text{(2a)}\\
\boldsymbol{W}_h^E &= \{\boldsymbol{t} \in \boldsymbol{L}^2(\mathcal{T}_E) : \boldsymbol{t}|_K \in \boldsymbol{\mathcal{P}}_k(K)\,, \quad \forall K \in \mathcal{T}_E\}, && \text{(2b)}\\
\underline{\boldsymbol{A}}_h &= \{\boldsymbol{\eta} \in \underline{\boldsymbol{L}}^2(\mathcal{T}_E) : \boldsymbol{\eta}|_K \in \underline{\boldsymbol{A}}(K)\,, \quad \forall K \in \mathcal{T}_E\}, && \text{(2c)}\\
\boldsymbol{M}_h &= \{\boldsymbol{\mu} \in \boldsymbol{L}^2(\mathcal{E}_E) : \boldsymbol{\mu}|_F \in \boldsymbol{\mathcal{P}}_k(F)\,, \quad \forall F \in \mathcal{E}_E\}, && \text{(2d)}\\
\boldsymbol{W}_h^A &= \{\boldsymbol{r} \in \boldsymbol{L}^2(\mathcal{T}_A) : \boldsymbol{r}|_K \in \boldsymbol{\mathcal{P}}_k(K)\,, \quad \forall K \in \mathcal{T}_A\}, && \text{(2e)}\\
W_h &= \{w \in L^2(\mathcal{T}_A) : w|_K \in \mathcal{P}_k(K)\,, \quad \forall K \in \mathcal{T}_A\}, && \text{(2f)}\\
M_h &= \{\xi \in L^2(\mathcal{E}_A) : \xi|_F \in \mathcal{P}_k(F)\,, \quad \forall F \in \mathcal{E}_A\}. && \text{(2g)}
\end{aligned}$$

The HDG discretization seeks a piecewise polynomial approximation

$$(\boldsymbol{\sigma}_h, \boldsymbol{u}_h, \boldsymbol{\gamma}_h, \widehat{\boldsymbol{u}}_h, \boldsymbol{q}_h, v_h, \widehat{v}_h) \in \underline{\boldsymbol{V}}_h \times \boldsymbol{W}_h^E \times \underline{\boldsymbol{A}}_h \times \boldsymbol{M}_h \times \boldsymbol{W}_h^A \times W_h \times M_h$$

of the exact solution $(\boldsymbol{\sigma}, \boldsymbol{u}, \boldsymbol{\gamma}, \boldsymbol{u}|_{\mathcal{E}_E}, \boldsymbol{q}, v, v|_{\mathcal{E}_A})$. The approximation must satisfy the discrete weak formulation

$$\begin{aligned}
(\mathbf{C}^{-1}\boldsymbol{\sigma}_h, \boldsymbol{\tau})_{\mathcal{T}_E} + (\boldsymbol{u}_h, \nabla\cdot\boldsymbol{\tau})_{\mathcal{T}_E} + (\boldsymbol{\gamma}_h, \boldsymbol{\tau})_{\mathcal{T}_E} - \langle \widehat{\boldsymbol{u}}_h, \boldsymbol{\tau}\boldsymbol{n}\rangle_{\partial\mathcal{T}_E} &= 0, && \text{(3a)}\\
(\boldsymbol{\sigma}_h, \nabla\boldsymbol{t})_{\mathcal{T}_E} - \langle \widehat{\boldsymbol{\sigma}}_h\boldsymbol{n}, \boldsymbol{t}\rangle_{\partial\mathcal{T}_E} + \rho_E s^2(\boldsymbol{u}_h, \boldsymbol{t})_{\mathcal{T}_E} &= (\boldsymbol{f}, \boldsymbol{t})_{\mathcal{T}_E}, && \text{(3b)}\\
(\boldsymbol{\sigma}_h, \boldsymbol{\eta})_{\mathcal{T}_E} &= 0, && \text{(3c)}\\
\langle \widehat{\boldsymbol{\sigma}}_h\boldsymbol{n}, \boldsymbol{\mu}\rangle_{\partial\mathcal{T}_E\setminus\Gamma} &= 0, && \text{(3d)}\\
(\boldsymbol{q}_h, \boldsymbol{r})_{\mathcal{T}_A} + (v_h, \nabla\cdot\boldsymbol{r})_{\mathcal{T}_A} - \langle \widehat{v}_h, \boldsymbol{r}\cdot\boldsymbol{n}\rangle_{\partial\mathcal{T}_A} &= 0, && \text{(3e)}\\
(\boldsymbol{q}_h, \nabla w)_{\mathcal{T}_A} - \langle \widehat{\boldsymbol{q}}_h\cdot\boldsymbol{n}, w\rangle_{\partial\mathcal{T}_A} + (s/c)^2(v_h, w)_{\mathcal{T}_A} &= (f, w)_{\mathcal{T}_A}, && \text{(3f)}\\
\langle \widehat{\boldsymbol{q}}_h\cdot\boldsymbol{n}, \xi\rangle_{\partial\mathcal{T}_A\setminus(\Gamma\cup\Gamma_A^D)} &= \langle g_N, \xi\rangle_{\Gamma_A^N}, && \text{(3g)}\\
\langle \widehat{v}_h, \xi\rangle_{\Gamma_A^D} &= \langle g_D, \xi\rangle_{\Gamma_A^D}, && \text{(3h)}\\
\langle \widehat{\boldsymbol{q}}_h\cdot\boldsymbol{n}_A - s\,\widehat{\boldsymbol{u}}_h\cdot\boldsymbol{n}_E, \xi\rangle_\Gamma &= -\langle \nabla v^{\text{inc}}\cdot\boldsymbol{n}_A, \xi\rangle_\Gamma, && \text{(3i)}\\
\langle -\widehat{\boldsymbol{\sigma}}_h\boldsymbol{n}_E + \rho_f s\,\widehat{v}_h\,\boldsymbol{n}_A, \boldsymbol{\mu}\rangle_\Gamma &= -\rho_f s\,\langle v^{\text{inc}}\,\boldsymbol{n}_A, \boldsymbol{\mu}\rangle_\Gamma && \text{(3j)}
\end{aligned}$$

for all test functions $(\boldsymbol{\tau}, \boldsymbol{t}, \boldsymbol{\eta}, \boldsymbol{\mu}, \boldsymbol{r}, w, \xi) \in \underline{\boldsymbol{V}}_h \times \boldsymbol{W}_h^E \times \underline{\boldsymbol{A}}_h \times \boldsymbol{M}_h \times \boldsymbol{W}_h^A \times W_h \times M_h$, where

$$\begin{aligned}
\widehat{\boldsymbol{\sigma}}_h\boldsymbol{n} &:= \boldsymbol{\sigma}_h\boldsymbol{n} - \tau_E(\boldsymbol{u}_h - \widehat{\boldsymbol{u}}_h) \qquad \text{on} \quad \partial\mathcal{T}_E, && \text{(3k)}\\
\widehat{\boldsymbol{q}}_h\cdot\boldsymbol{n} &:= \boldsymbol{q}_h\cdot\boldsymbol{n} - \tau_A(v_h - \widehat{v}_h) \qquad \text{on} \quad \partial\mathcal{T}_A. && \text{(3l)}
\end{aligned}$$

Here, τ_E and τ_A are stabilization parameters whose properties will be determined when analyzing the scheme.

4 Discrete well posedness.

Theorem 4.1. *If* $\mathrm{Re}(s\tau_A) > 0$ *and* $\mathrm{Re}(s\tau_E) > 0$*, then the scheme* (3) *has a unique solution.*

Proof. By the Fredholm alternative, it is enough to show uniqueness of the solution. To that end, if we assume zero sources, we will show that the solution to the corresponding system is the trivial one.

Let

$$v^{\text{inc}} = 0 \qquad \text{and} \qquad (f, \boldsymbol{f}, g_D, g_N) = (0, \mathbf{0}, 0, 0),$$

and choose

$$(\boldsymbol{\tau}, \boldsymbol{t}, \boldsymbol{\eta}, \boldsymbol{\mu}, \boldsymbol{r}, w) = (\widehat{\boldsymbol{\sigma}}_h, \boldsymbol{u}_h, \boldsymbol{\gamma}_h, \widehat{\boldsymbol{u}}_h, \boldsymbol{q}_h, v_h) \qquad \text{and} \qquad \xi = \left\{ \begin{array}{ll} \widehat{v}_h, & \text{on } \partial\mathcal{T}_A\setminus\Gamma_A^D \\ \widehat{\boldsymbol{q}}_h\cdot\boldsymbol{n}, & \text{on } \Gamma_A^D \end{array} \right. .$$

With this choice of test functions, applying integration by parts to (3b) and adding its conjugate to (3a) we obtain

$$\begin{aligned}
&(\mathbf{C}^{-1}\boldsymbol{\sigma}_h,\boldsymbol{\sigma}_h)_{\mathcal{T}_E} + (\boldsymbol{u}_h,\nabla\cdot\boldsymbol{\sigma}_h)_{\mathcal{T}_E} + (\boldsymbol{\gamma}_h,\boldsymbol{\sigma}_h)_{\mathcal{T}_E} - \langle\widehat{\boldsymbol{u}}_h,\boldsymbol{\sigma}_h\boldsymbol{n}\rangle_{\partial\mathcal{T}_E}\\
&-\overline{(\nabla\cdot\boldsymbol{\sigma}_h,\boldsymbol{u}_h)_{\mathcal{T}_E}} + \overline{\langle\boldsymbol{\sigma}_h\boldsymbol{n},\boldsymbol{u}_h\rangle_{\partial\mathcal{T}_E}} - \overline{\langle\widehat{\boldsymbol{\sigma}}_h\boldsymbol{n},\boldsymbol{u}_h\rangle_{\partial\mathcal{T}_E}} + \rho_E\overline{s^2}(\boldsymbol{u}_h,\boldsymbol{u}_h)_{\mathcal{T}_E} = 0.
\end{aligned}$$

We know from (3c) that $(\boldsymbol{\sigma}_h,\boldsymbol{\gamma}_h)_{\mathcal{T}_E}=0$, so the latter equation becomes

$$(\mathbf{C}^{-1}\boldsymbol{\sigma}_h,\boldsymbol{\sigma}_h)_{\mathcal{T}_E} + \overline{\langle\boldsymbol{\sigma}_h\boldsymbol{n}-\widehat{\boldsymbol{\sigma}}_h\boldsymbol{n},\boldsymbol{u}_h\rangle_{\partial\mathcal{T}_E}} - \langle\widehat{\boldsymbol{u}}_h,\boldsymbol{\sigma}_h\boldsymbol{n}\rangle_{\partial\mathcal{T}_E} + \rho_E\overline{s^2}(\boldsymbol{u}_h,\boldsymbol{u}_h)_{\mathcal{T}_E} = 0.$$

Adding and subtracting $\widehat{\boldsymbol{u}}_h$ in the second argument of the second term, we have that

$$\begin{aligned}
&\|\boldsymbol{\sigma}_h\|^2_{\mathcal{T}_E,\mathbf{C}^{-1}} + \overline{\langle\boldsymbol{\sigma}_h\boldsymbol{n}-\widehat{\boldsymbol{\sigma}}_h\boldsymbol{n},\boldsymbol{u}_h-\widehat{\boldsymbol{u}}_h\rangle_{\partial\mathcal{T}_E}} + \overline{\langle\boldsymbol{\sigma}_h\boldsymbol{n}-\widehat{\boldsymbol{\sigma}}_h\boldsymbol{n},\widehat{\boldsymbol{u}}_h\rangle_{\partial\mathcal{T}_E}}\\
&\qquad - \langle\widehat{\boldsymbol{u}}_h,\boldsymbol{\sigma}_h\boldsymbol{n}\rangle_{\partial\mathcal{T}_E} + \rho_E\overline{s^2}\,\|\boldsymbol{u}_h\|^2_{\mathcal{T}_E} = 0.
\end{aligned}$$

Multiplying by s and using (3d), along with the definition (3k), we obtain

$$s\,\|\boldsymbol{\sigma}_h\|^2_{\mathcal{T}_E,\mathbf{C}^{-1}} + s\overline{\langle\tau_E(\boldsymbol{u}_h-\widehat{\boldsymbol{u}}_h),\boldsymbol{u}_h-\widehat{\boldsymbol{u}}_h\rangle_{\partial\mathcal{T}_E}} - s\langle\widehat{\boldsymbol{u}}_h,\widehat{\boldsymbol{\sigma}}_h\boldsymbol{n}_E\rangle_\Gamma + \rho_E\overline{s}|s|^2\,\|\boldsymbol{u}_h\|^2_{\mathcal{T}_E} = 0. \tag{4}$$

Analogously for the acoustic terms, (3f) is integrated by parts and its conjugate is added to (3e), yielding

$$\begin{aligned}
&\|\boldsymbol{q}_h\|^2_{\mathcal{T}_A} + (v_h,\nabla\cdot\boldsymbol{q}_h)_{\mathcal{T}_A} - \langle v_h,\boldsymbol{q}_h\cdot\boldsymbol{n}\rangle_{\partial\mathcal{T}_A} - \overline{(\nabla\cdot\boldsymbol{q}_h,v_h)_{\mathcal{T}_A}}\\
&\qquad + \overline{\langle\boldsymbol{q}_h\cdot\boldsymbol{n},v_h\rangle_{\partial\mathcal{T}_A}} - \overline{\langle\widehat{\boldsymbol{q}}_h\cdot\boldsymbol{n},v_h\rangle_{\partial\mathcal{T}_A}} + \frac{\overline{s^2}}{c^2}\,\|v_h\|^2_{\mathcal{T}_A} = 0.
\end{aligned}$$

Adding and subtracting $\widehat{v}_h$ and using (3g) and (3h), we can deduce that

$$\|\boldsymbol{q}_h\|^2_{\mathcal{T}_A} + \overline{\langle\tau_A(v_h-\widehat{v}_h),v_h-\widehat{v}_h\rangle_{\partial\mathcal{T}_A}} - \langle\widehat{v}_h,\widehat{\boldsymbol{q}}_h\cdot\boldsymbol{n}_A\rangle_\Gamma + \frac{\overline{s^2}}{c^2}\,\|v_h\|^2_{\mathcal{T}_A} = 0.$$

We multiply the latter equation by $\rho_f s$ to obtain

$$\rho_f s\,\|\boldsymbol{q}_h\|^2_{\mathcal{T}_A} + \rho_f s\overline{\langle\tau_A(v_h-\widehat{v}_h),v_h-\widehat{v}_h\rangle_{\partial\mathcal{T}_A}} - \rho_f s\langle\widehat{v}_h,\widehat{\boldsymbol{q}}_h\cdot\boldsymbol{n}_A\rangle_\Gamma + \rho_f\overline{s}(|s|/c)^2\,\|v_h\|^2_{\mathcal{T}_A} = 0. \tag{5}$$

Adding (4) with the conjugate of (5) leads to

$$\begin{aligned}
&s\,\|\boldsymbol{\sigma}_h\|^2_{\mathcal{T}_E,\mathbf{C}^{-1}} + s\overline{\langle\tau_E(\boldsymbol{u}_h-\widehat{\boldsymbol{u}}_h),\boldsymbol{u}_h-\widehat{\boldsymbol{u}}_h\rangle_{\partial\mathcal{T}_E}} - s\langle\widehat{\boldsymbol{u}}_h,\widehat{\boldsymbol{\sigma}}_h\boldsymbol{n}_E\rangle_\Gamma + \rho_E\overline{s}|s|^2\,\|\boldsymbol{u}_h\|^2_{\mathcal{T}_E}\\
&+\rho_f\overline{s}\,\|\boldsymbol{q}_h\|^2_{\mathcal{T}_A} + \rho_f\overline{s}\langle\tau_A(v_h-\widehat{v}_h),v_h-\widehat{v}_h\rangle_{\partial\mathcal{T}_A} - \rho_f\overline{s}\overline{\langle\widehat{v}_h,\widehat{\boldsymbol{q}}_h\cdot\boldsymbol{n}_A\rangle_\Gamma} + \rho_f\overline{s}(|s|/c)^2\,\|v_h\|^2_{\mathcal{T}_A} = 0
\end{aligned} \tag{6}$$

Notice that from (3i) and (3j) we have

$$\begin{aligned}
-s\langle\widehat{\boldsymbol{u}}_h,\widehat{\boldsymbol{\sigma}}_h\boldsymbol{n}_E\rangle_\Gamma - \rho_f\overline{s}\overline{\langle\widehat{v}_h,\widehat{\boldsymbol{q}}_h\cdot\boldsymbol{n}_A\rangle_\Gamma} &= -\,s\langle\widehat{\boldsymbol{u}}_h,\widehat{\boldsymbol{\sigma}}_h\boldsymbol{n}_E-\rho_f s\widehat{v}_h\boldsymbol{n}_A\rangle_\Gamma - s\langle\widehat{\boldsymbol{u}}_h,\rho_f s\widehat{v}_h\boldsymbol{n}_A\rangle_\Gamma\\
&\quad - \rho_f\overline{s}\overline{\langle\widehat{v}_h,\widehat{\boldsymbol{q}}_h\cdot\boldsymbol{n}_A-s\widehat{\boldsymbol{u}}_h\cdot\boldsymbol{n}_E\rangle_\Gamma} - \rho_f\overline{s}\overline{\langle\widehat{v}_h,s\widehat{\boldsymbol{u}}_h\cdot\boldsymbol{n}_E\rangle_\Gamma}\\
&= -\,s\langle\widehat{\boldsymbol{u}}_h,\rho_f s\widehat{v}_h\boldsymbol{n}_A\rangle_\Gamma - \rho_f\overline{s}\overline{\langle\widehat{v}_h,s\widehat{\boldsymbol{u}}_h\cdot\boldsymbol{n}_E\rangle_\Gamma}\\
&= -\,s\overline{s}\rho_f\langle\widehat{\boldsymbol{u}}_h,\widehat{v}_h\boldsymbol{n}_A\rangle_\Gamma + s\overline{s}\rho_f\langle\widehat{\boldsymbol{u}}_h,\widehat{v}_h\boldsymbol{n}_A\rangle_\Gamma = 0.
\end{aligned}$$

So, (6) is equivalent to

$$\begin{aligned}
&s\,\|\boldsymbol{\sigma}_h\|^2_{\mathcal{T}_E,\mathbf{C}^{-1}} + s\overline{\langle\tau_E(\boldsymbol{u}_h-\widehat{\boldsymbol{u}}_h),\boldsymbol{u}_h-\widehat{\boldsymbol{u}}_h\rangle_{\partial\mathcal{T}_E}} + \rho_E\overline{s}|s|^2\,\|\boldsymbol{u}_h\|^2_{\mathcal{T}_E}\\
&+\rho_f\overline{s}\,\|\boldsymbol{q}_h\|^2_{\mathcal{T}_A} + \rho_f\overline{s}\langle\tau_A(v_h-\widehat{v}_h),v_h-\widehat{v}_h\rangle_{\partial\mathcal{T}_A} + \rho_f s(|s|/c)^2\,\|v_h\|^2_{\mathcal{T}_A} = 0.
\end{aligned}$$

Thus, taking real part of this expression, we obtain

$$\mathscr{E}_E^2 + \mathscr{E}_A^2 + \rho_E|s|^2\mathrm{Re}(s)\,\|\boldsymbol{u}_h\|^2_{\mathcal{T}_E} + \frac{\rho_f}{c^2}|s|^2\mathrm{Re}(s)\,\|v_h\|^2_{\mathcal{T}_A} = 0\,,$$

where we have defined

$$\begin{aligned}
\mathscr{E}_E &:= \sqrt{\left\|\mathrm{Re}(s)^{1/2}\,\boldsymbol{\sigma}_h\right\|^2_{\mathcal{T}_E,\mathbf{C}^{-1}} + \left\|\mathrm{Re}(s\tau_E)^{1/2}\,(\boldsymbol{u}_h-\widehat{\boldsymbol{u}}_h)\right\|^2_{\partial\mathcal{T}_E}}\\
\mathscr{E}_A &:= \sqrt{\left\|\rho_f^{1/2}\mathrm{Re}(s)^{1/2}\,\boldsymbol{q}_h\right\|^2_{\mathcal{T}_A} + \left\|\rho_f^{1/2}\mathrm{Re}(s\tau_A)^{1/2}\,(v_h-\widehat{v}_h)\right\|^2_{\partial\mathcal{T}_A}}.
\end{aligned}$$

From here, we can conclude that $\boldsymbol{\sigma}_h = \mathbf{0}$ in $\mathcal{T}_E$, $\boldsymbol{u}_h = \mathbf{0}$ in $\mathcal{T}_E$, $\boldsymbol{q}_h = \mathbf{0}$ in $\mathcal{T}_A$, $v_h = 0$ in $\mathcal{T}_A$, $\widehat{\boldsymbol{u}}_h = \boldsymbol{u}_h = \mathbf{0}$ on $\partial\mathcal{T}_E$ and $\widehat{v}_h = v_h = 0$ on $\partial\mathcal{T}_A$.

It only remains to show that $\boldsymbol{\gamma}_h = \mathbf{0}$ in $\mathcal{T}_E$. This will be achieved by performing an analog of the steps done in the proof of [7, Lemma 3.6]. We will need the two following technical results proven in [33]:

1. [33, Lemma 2.8] Given $\boldsymbol{\eta} \in \underline{\boldsymbol{A}}_h^0 := \{\boldsymbol{\eta} \in \underline{\boldsymbol{A}}_h : (\boldsymbol{\eta}, \boldsymbol{v})_K = 0, \forall \boldsymbol{v} \in \underline{\boldsymbol{\mathcal{P}}}_0(K)\,, \forall K \in \mathcal{T}_E\}$, there exists $\boldsymbol{v} \in \underline{\boldsymbol{\mathcal{B}}}_h$ such that
$$\boldsymbol{P}\boldsymbol{v} = \boldsymbol{\eta} \quad \text{ and } \quad \|\boldsymbol{v}\|_{\mathcal{T}_E} \leq C^0 \|\boldsymbol{\eta}\|_{\mathcal{T}_E}\,.$$
Here $\boldsymbol{P} : \underline{\boldsymbol{L}}^2(\Omega_E) \to \underline{\boldsymbol{A}}_h$ is the L^2-projection onto $\underline{\boldsymbol{A}}_h$ and C^0 is a positive constant independent of h, arising from a Poincaré-type inequality and inverse estimates.

2. [33, Proposition 2.9] Given $\boldsymbol{\eta} \in \underline{\boldsymbol{A}}_h^c := \underline{\boldsymbol{A}}_h \cap \underline{\boldsymbol{\mathcal{P}}}_0(\mathcal{T}_E)$, there exists $\boldsymbol{v} \in \underline{\boldsymbol{H}}(\text{div};\Omega_E) \cap \underline{\boldsymbol{\mathcal{P}}}_1(\mathcal{T}_E)$ such that
$$\nabla\cdot\boldsymbol{v} = 0\,, \qquad \boldsymbol{P}^c\boldsymbol{v} = \boldsymbol{\eta}\,, \qquad \text{and} \qquad \|\boldsymbol{v}\|_{\mathcal{T}_E} \leq C^c \|\boldsymbol{\eta}\|_{\mathcal{T}_E}\,, \tag{7}$$
where $\boldsymbol{P}^c$ is the L^2-projection onto $\underline{\boldsymbol{A}}_h^c$, and $C^c > 0$ is a constant independent of h.

Let us consider the orthogonal decomposition
$$\boldsymbol{\gamma}_h = \boldsymbol{\gamma}_h^0 + \boldsymbol{\gamma}_h^c \quad \text{where} \quad \boldsymbol{\gamma}_h^c|_K := \frac{1}{|K|}\int_K \boldsymbol{\gamma}_h, \forall K \in \mathcal{T}_E \quad \text{(component-wise)} \quad \text{and} \quad \boldsymbol{\gamma}_h^0 = \boldsymbol{\gamma}_h - \boldsymbol{\gamma}_h^c.$$

It is clear that $\boldsymbol{\gamma}_h^0 \in \underline{\boldsymbol{A}}_h^0$ and $\boldsymbol{\gamma}_h^c \in \underline{\boldsymbol{A}}_h^c$.

By [33, Lemma 3.9], there exists
$$\boldsymbol{v}^0 \in \underline{\boldsymbol{\mathcal{B}}_h} := \{\boldsymbol{\eta} \in \underline{\boldsymbol{L}}^2(\Omega_E) : \boldsymbol{\eta}|_K \in \underline{\boldsymbol{B}}(K)\,, K \in \mathcal{T}_E\} \subset \underline{\boldsymbol{V}}_h$$
such that
$$(\boldsymbol{\gamma}_h^0, \boldsymbol{\rho}^0)_{\mathcal{T}_E} = (\boldsymbol{v}^0, \boldsymbol{\rho}^0)_{\mathcal{T}_E} \quad \text{for all } \boldsymbol{\rho}^0 \in \underline{\boldsymbol{A}}_h. \tag{8}$$
Taking $\boldsymbol{\tau} = \boldsymbol{v}^0$ in (3a), we obtain
$$(\boldsymbol{\gamma}_h^0 + \boldsymbol{\gamma}_h^c, \boldsymbol{v}^0)_{\mathcal{T}_E} = 0.$$
Now, considering $\boldsymbol{\rho}^0 = \boldsymbol{\gamma}_h^c$, and the fact that the decomposition of $\boldsymbol{\gamma}_h$ is orthogonal in $\underline{\boldsymbol{L}}^2$, the two expressions above imply
$$(\boldsymbol{\gamma}_h^0, \boldsymbol{v}^0)_{\mathcal{T}_E} = (\boldsymbol{\gamma}_h^0, \boldsymbol{\gamma}_h^c)_{\mathcal{T}_E} = 0.$$
Hence, taking $\boldsymbol{\rho}^0 = \boldsymbol{\gamma}_h^0$ in (8), the equality above shows that $(\boldsymbol{\gamma}_h^0, \boldsymbol{v}^0)_{\mathcal{T}_E} = \|\boldsymbol{\gamma}_h^0\|^2_{\mathcal{T}_E} = 0$, and we can conclude that $\boldsymbol{\gamma}_h^0 = \mathbf{0}$.

Finally, by the second property in (7), there exists $\boldsymbol{v}^c \in \underline{\boldsymbol{H}}(\text{div};\Omega_E) \cap \underline{\boldsymbol{\mathcal{P}}}_1(\mathcal{T}_E)$ such that
$$(\boldsymbol{v}^c, \boldsymbol{\rho}^c)_{\mathcal{T}_E} = (\boldsymbol{\gamma}_h^c, \boldsymbol{\rho}^c)_{\mathcal{T}_E} \quad \text{for all } \boldsymbol{\rho}^c \in \underline{\boldsymbol{A}}_h^c.$$

Taking $\boldsymbol{\rho}^c = \boldsymbol{\gamma}_h^c$ in the expression above we have
$$(\boldsymbol{\gamma}_h^c, \boldsymbol{v}^c)_{\mathcal{T}_E} = \|\boldsymbol{\gamma}_h^c\|^2_{\mathcal{T}_E}\,. \tag{9}$$

Now, recalling that $\boldsymbol{\sigma}_h = \mathbf{0}$ and $\boldsymbol{u}_h = \mathbf{0}$ in $\mathcal{T}_E$ and $\widehat{\boldsymbol{u}}_h = \mathbf{0}$ on $\partial\mathcal{T}_E$, choosing $\boldsymbol{\tau} = \boldsymbol{v}^c$ in (3a), we have that $(\boldsymbol{\gamma}_h, \boldsymbol{v}^c)_{\mathcal{T}_E} = 0$. Then, since $\boldsymbol{\gamma}_h^0 = \mathbf{0}$, from (9) we conclude $\boldsymbol{\gamma}_h^c = \mathbf{0}$ in $\mathcal{T}_E$, and therefore $\boldsymbol{\gamma}_h = 0$. □

5 Error Analysis.

5.1 The HDG Projections.

We will need the HDG projections defined in [18]. For the acoustic terms, the projected function is denoted by $\boldsymbol{\Pi_A}(\boldsymbol{q}, v) := (\boldsymbol{\Pi_A}\boldsymbol{q}, \Pi_A v)$, where $\boldsymbol{\Pi_A}\boldsymbol{q}$ and $\Pi_A v$ are the components of the projection in $\boldsymbol{W}_h^A$ and W_h, respectively.

The values of the projection on any simplex $K \in \mathcal{T}_A$ are fixed when the components are required to satisfy the equations

$$\begin{aligned}
(\boldsymbol{\Pi_A q}, \boldsymbol{r})_K &= (\boldsymbol{q}, \boldsymbol{r})_K, && \forall \boldsymbol{r} \in \boldsymbol{\mathcal{P}}_{k-1}(K)\,,\\
(\Pi_A v, w)_K &= (v, w)_K, && \forall w \in \mathcal{P}_{k-1}(K)\,,\\
\langle \boldsymbol{\Pi_A q} \cdot \boldsymbol{n} - \tau_A \Pi_A v, \xi \rangle_F &= \langle \boldsymbol{q} \cdot \boldsymbol{n} - \tau_A P_M v, \xi \rangle_F\,, && \forall \xi \in \mathcal{P}_k(F)\,,
\end{aligned}$$

for all faces F of the simplex $K \in \mathcal{T}_A$, where P_M is the L^2 projection onto F. It was shown in [18] that, if $(\boldsymbol{q}, v) \in \boldsymbol{H}^{k+1}(K) \times H^{k+1}(K)$ and $\tau_A|_{\partial K}$ is nonnegative and $\max\limits_{\partial K} \tau_A > 0$, the components of the projection satisfy the estimates

$$\|\boldsymbol{\Pi_A q} - \boldsymbol{q}\|_K \lesssim h_K^{k+1} \left(|\boldsymbol{q}|_{\boldsymbol{H}^{k+1}(K)} + |v|_{H^{k+1}(K)} \right), \tag{10a}$$

$$\|\Pi_A v - v\|_K \lesssim h_K^{k+1} \left(|v|_{H^{k+1}(K)} + |\nabla \cdot \boldsymbol{q}|_{H^k(K)} \right). \tag{10b}$$

Therefore, for the sake of simplicity, from now on we assume that τ_E and τ_A are positive functions.

For the elastic terms, on each element $K \in \mathcal{T}_E$, a component-wise version of the above projection is defined by $\boldsymbol{\Pi_E}(\boldsymbol{\sigma}, \boldsymbol{u}) := (\underline{\boldsymbol{\Pi}}_{\boldsymbol{E}} \boldsymbol{\sigma}, \boldsymbol{\Pi_E u}) \in \underline{\boldsymbol{\mathcal{P}}}_k(K) \times \boldsymbol{\mathcal{P}}_k(K)$ where

$$\begin{aligned}
(\underline{\boldsymbol{\Pi}}_{\boldsymbol{E}} \boldsymbol{\sigma}, \boldsymbol{\tau})_K &= (\boldsymbol{\sigma}, \boldsymbol{\tau})_K, && \forall \boldsymbol{\tau} \in \underline{\boldsymbol{\mathcal{P}}}_{k-1}(K)\,,\\
(\boldsymbol{\Pi_E u}, \boldsymbol{t})_K &= (\boldsymbol{u}, \boldsymbol{t})_K, && \forall \boldsymbol{t} \in \boldsymbol{\mathcal{P}}_{k-1}(K)\,,\\
\langle (\underline{\boldsymbol{\Pi}}_{\boldsymbol{E}} \boldsymbol{\sigma}) \boldsymbol{n} - \tau_E \boldsymbol{\Pi_E u}, \boldsymbol{\mu} \rangle_F &= \langle \boldsymbol{\sigma n} - \tau_E \boldsymbol{P_M u}, \boldsymbol{\mu} \rangle_F\,, && \forall \boldsymbol{\mu} \in \boldsymbol{\mathcal{P}}_k(F)\,,
\end{aligned}$$

for all faces F of the element $K \in \mathcal{T}_E$. Above, $\boldsymbol{P_M}$ is the $\boldsymbol{L}^2$ projection onto F. Analogously, if $(\boldsymbol{\sigma}, \boldsymbol{u}) \in \underline{\boldsymbol{H}}^{k+1}(K) \times \boldsymbol{H}^{k+1}(K)$, then

$$\|\underline{\boldsymbol{\Pi}}_{\boldsymbol{E}} \boldsymbol{\sigma} - \boldsymbol{\sigma}\|_K \lesssim h_K^{k+1} \left(|\boldsymbol{\sigma}|_{\underline{\boldsymbol{H}}^{k+1}(K)} + |\boldsymbol{u}|_{\boldsymbol{H}^{k+1}(K)} \right), \tag{11a}$$

$$\|\boldsymbol{\Pi_E u} - \boldsymbol{u}\|_K \lesssim h_K^{k+1} \left(|\boldsymbol{u}|_{\boldsymbol{H}^{k+1}(K)} + |\nabla \cdot \boldsymbol{\sigma}|_{\underline{\boldsymbol{H}}^k(K)} \right). \tag{11b}$$

In addition, for each element $K \in \mathcal{T}_E$, we will denote by $\underline{\boldsymbol{\Pi}} \boldsymbol{\gamma}$ the $\underline{\boldsymbol{L}}^2(K)$-projection of $\boldsymbol{\gamma}$ on $\underline{\boldsymbol{A}}(K)$. Thus, if $\boldsymbol{\gamma} \in \underline{\boldsymbol{H}}^{k+1}(K)$, then

$$\|\underline{\boldsymbol{\Pi}} \boldsymbol{\gamma} - \boldsymbol{\gamma}\|_K \lesssim h_K^{k+1} |\boldsymbol{\gamma}|_{\underline{\boldsymbol{H}}^{k+1}(K)}\,.$$

Having defined the projections, we now define the *projection errors* in each of the volume unknowns by

$$\begin{aligned}
&\boldsymbol{\delta_\sigma} := \boldsymbol{\sigma} - \underline{\boldsymbol{\Pi}}_{\boldsymbol{E}} \boldsymbol{\sigma}, \qquad \boldsymbol{\delta_u} := \boldsymbol{u} - \boldsymbol{\Pi_E u}, \qquad \boldsymbol{\delta_\gamma} := \boldsymbol{\gamma} - \underline{\boldsymbol{\Pi}} \boldsymbol{\gamma},\\
&\boldsymbol{\delta_q} := \boldsymbol{q} - \boldsymbol{\Pi_A q}, \qquad \delta_v := v - \Pi_A v.
\end{aligned}$$

The following quantity will play a fundamental role in the error estimations:

$$\Theta(\boldsymbol{\sigma}, \boldsymbol{u}, \boldsymbol{\gamma}, \boldsymbol{q}, v) := \left(\|\boldsymbol{\delta_\sigma}\|^2_{\mathcal{T}_E} + \|\boldsymbol{\delta_u}\|^2_{\mathcal{T}_E} + \|\boldsymbol{\delta_\gamma}\|^2_{\mathcal{T}_E} + \|\boldsymbol{\delta_q}\|^2_{\mathcal{T}_A} + \|\delta_v\|^2_{\mathcal{T}_A} \right)^{1/2}.$$

The next lemma follows readily from the projection bounds (10) and (11).

Lemma 5.1. *If* $(\boldsymbol{\sigma}, \boldsymbol{u}, \boldsymbol{\gamma}, \boldsymbol{q}, v) \in \underline{\boldsymbol{H}}^{k+1}(\Omega_E) \times \boldsymbol{H}^{k+1}(\Omega_E) \times \underline{\boldsymbol{H}}^{k+1}(\Omega_E) \times \boldsymbol{H}^{k+1}(\Omega_A) \times H^{k+1}(\Omega_A)$*, then*

$$\Theta(\boldsymbol{\sigma}, \boldsymbol{u}, \boldsymbol{\gamma}, \boldsymbol{q}, v) \lesssim h^{k+1} \left(|\boldsymbol{\sigma}|_{\underline{\boldsymbol{H}}^{k+1}(\Omega_E)} + |\boldsymbol{u}|_{\boldsymbol{H}^{k+1}(\Omega_E)} + |\boldsymbol{\gamma}|_{\underline{\boldsymbol{H}}^{k+1}(\Omega_E)} + |\boldsymbol{q}|_{\boldsymbol{H}^{k+1}(\Omega_A)} + |v|_{H^{k+1}(\Omega_A)} \right).$$

5.2 Error estimates.

Let us define the *projections of the errors* (not to be confused with the projection errors defined above):

$$\begin{aligned}
&\boldsymbol{e_\sigma} := \underline{\boldsymbol{\Pi}}_{\boldsymbol{E}} \boldsymbol{\sigma} - \boldsymbol{\sigma}_h, && \boldsymbol{e_{\widehat{\sigma}} n} := \boldsymbol{P_M}(\boldsymbol{\sigma n}) - \widehat{\boldsymbol{\sigma}}_h \boldsymbol{n}, && \boldsymbol{e_u} := \boldsymbol{\Pi_E u} - \boldsymbol{u}_h,\\
&\boldsymbol{e_{\widehat{u}}} := \boldsymbol{P_M u} - \widehat{\boldsymbol{u}}_h, && \boldsymbol{e_\gamma} := \underline{\boldsymbol{\Pi}} \boldsymbol{\gamma} - \boldsymbol{\gamma}_h, && \boldsymbol{e_q} := \boldsymbol{\Pi_A q} - \boldsymbol{q}_h,\\
&\boldsymbol{e_{\widehat{q}}} \cdot \boldsymbol{n} := P_M(\boldsymbol{q} \cdot \boldsymbol{n}) - \boldsymbol{q}_h \cdot \boldsymbol{n}, && e_v := \Pi_A v - v_h, && e_{\widehat{v}} := P_M v - \widehat{v}_h.
\end{aligned}$$

Direct calculations imply that, for all $(\boldsymbol{\tau},\boldsymbol{t},\boldsymbol{\eta},\boldsymbol{\mu},\boldsymbol{r},w,\xi)\in \underline{\boldsymbol{V}}_h\times \boldsymbol{W}_h^E\times \underline{\boldsymbol{A}}_h\times \boldsymbol{M}_h\times \boldsymbol{W}_h^A\times W_h\times M_h$, the projections of the errors satisfy the following system:

$$(\mathbf{C}^{-1}\boldsymbol{e}_{\boldsymbol{\sigma}},\boldsymbol{\tau})_{\mathcal{T}_E}+(\boldsymbol{e}_{\boldsymbol{u}},\nabla\cdot\boldsymbol{\tau})_{\mathcal{T}_E}+(\boldsymbol{e}_{\boldsymbol{\gamma}},\boldsymbol{\tau})_{\mathcal{T}_E}-\langle \boldsymbol{e}_{\widehat{\boldsymbol{u}}},\boldsymbol{\tau}\boldsymbol{n}\rangle_{\partial\mathcal{T}_E}=-(\mathbf{C}^{-1}\boldsymbol{\delta}_{\boldsymbol{\sigma}},\boldsymbol{\tau})_{\mathcal{T}_E}-(\boldsymbol{\delta}_{\boldsymbol{\gamma}},\boldsymbol{\tau})_{\mathcal{T}_E}, \tag{12a}$$

$$(\boldsymbol{e}_{\boldsymbol{\sigma}},\nabla\boldsymbol{t})_{\mathcal{T}_E}-\langle \boldsymbol{e}_{\widehat{\boldsymbol{\sigma}}}\boldsymbol{n},\boldsymbol{t}\rangle_{\partial\mathcal{T}_E}+\rho_E s^2(\boldsymbol{e}_{\boldsymbol{u}},\boldsymbol{t})_{\mathcal{T}_E}=-\rho_E s^2(\boldsymbol{\delta}_{\boldsymbol{u}},\boldsymbol{t})_{\mathcal{T}_E}, \tag{12b}$$

$$(\boldsymbol{e}_{\boldsymbol{\sigma}},\boldsymbol{\eta})_{\mathcal{T}_E}=-(\boldsymbol{\delta}_{\boldsymbol{\sigma}},\boldsymbol{\eta})_{\mathcal{T}_E}, \tag{12c}$$

$$\langle \boldsymbol{e}_{\widehat{\boldsymbol{\sigma}}}\boldsymbol{n},\boldsymbol{\mu}\rangle_{\partial\mathcal{T}_E\setminus\Gamma}=0, \tag{12d}$$

$$(\boldsymbol{e}_{\boldsymbol{q}},\boldsymbol{r})_{\mathcal{T}_A}+(e_v,\nabla\cdot\boldsymbol{r})_{\mathcal{T}_A}-\langle e_{\widehat{v}},\boldsymbol{r}\cdot\boldsymbol{n}\rangle_{\partial\mathcal{T}_A}=-(\boldsymbol{\delta}_{\boldsymbol{q}},\boldsymbol{r})_{\mathcal{T}_A}, \tag{12e}$$

$$(\boldsymbol{e}_{\boldsymbol{q}},\nabla w)_{\mathcal{T}_A}-\langle \boldsymbol{e}_{\widehat{\boldsymbol{q}}}\cdot\boldsymbol{n},w\rangle_{\partial\mathcal{T}_A}+(s/c)^2(e_v,w)_{\mathcal{T}_A}=-(s/c)^2(\delta_v,w)_{\mathcal{T}_A}, \tag{12f}$$

$$\langle \boldsymbol{e}_{\widehat{\boldsymbol{q}}}\cdot\boldsymbol{n},\xi\rangle_{\partial\mathcal{T}_A\setminus(\Gamma\cup\Gamma_A^D)}=0, \tag{12g}$$

$$\langle e_{\widehat{v}},\xi\rangle_{\Gamma_A^D}=0, \tag{12h}$$

$$\langle \boldsymbol{e}_{\widehat{\boldsymbol{q}}}\cdot\boldsymbol{n}_A-s\,\boldsymbol{e}_{\widehat{\boldsymbol{u}}}\cdot\boldsymbol{n}_E,\xi\rangle_{\Gamma}=0, \tag{12i}$$

$$\langle -\boldsymbol{e}_{\widehat{\boldsymbol{\sigma}}}\boldsymbol{n}_E+\rho_f s\, e_{\widehat{v}}\,\boldsymbol{n}_A,\boldsymbol{\mu}\rangle_{\Gamma}=0 \tag{12j}$$

while $\boldsymbol{e}_{\widehat{\boldsymbol{\sigma}}}$ and $\boldsymbol{e}_{\widehat{\boldsymbol{q}}}$ satisfy

$$\boldsymbol{e}_{\widehat{\boldsymbol{\sigma}}}\boldsymbol{n}=\boldsymbol{e}_{\boldsymbol{\sigma}}\boldsymbol{n}-\tau_E(\boldsymbol{e}_{\boldsymbol{u}}-\boldsymbol{e}_{\widehat{\boldsymbol{u}}})\quad \text{on } \partial\mathcal{T}_E, \tag{12k}$$

$$\boldsymbol{e}_{\widehat{\boldsymbol{q}}}\cdot\boldsymbol{n}=\boldsymbol{e}_{\boldsymbol{q}}\cdot\boldsymbol{n}-\tau_A(e_v-e_{\widehat{v}})\quad \text{on } \partial\mathcal{T}_A. \tag{12l}$$

The following lemma can be proven by arguing as in the first part of the proof of Theorem 4.1.

Lemma 5.2. *The projections of the errors satisfy*

$$\begin{aligned}
e_E^2+e_A^2+\rho_E|s|^2\mathrm{Re}(s)\,\|\boldsymbol{e}_{\boldsymbol{u}}\|^2_{\mathcal{T}_E}+\frac{\rho_f}{c^2}|s|^2\mathrm{Re}(s)\,\|e_v\|^2_{\mathcal{T}_A}&\\
=-\mathrm{Re}\big(s(\mathbf{C}^{-1}\boldsymbol{\delta}_{\boldsymbol{\sigma}},\boldsymbol{e}_{\boldsymbol{\sigma}})_{\mathcal{T}_E}\big)&+\mathrm{Re}(s(\boldsymbol{e}_{\boldsymbol{\gamma}},\boldsymbol{\delta}_{\boldsymbol{\sigma}})_{\mathcal{T}_E})-\mathrm{Re}(s(\boldsymbol{\delta}_{\boldsymbol{\gamma}},\boldsymbol{e}_{\boldsymbol{\sigma}})_{\mathcal{T}_E})\\
-\rho_E|s|^2\mathrm{Re}(s(\boldsymbol{e}_{\boldsymbol{u}},\boldsymbol{\delta}_{\boldsymbol{u}})_{\mathcal{T}_E})&-\rho_f\mathrm{Re}(\overline{s}(\boldsymbol{e}_{\boldsymbol{q}},\boldsymbol{\delta}_{\boldsymbol{q}})_{\mathcal{T}_A})-\frac{\rho_f}{c^2}|s|^2\mathrm{Re}(s(\delta_v,e_v)_{\mathcal{T}_A})\,,
\end{aligned} \tag{13}$$

where

$$e_E:=\sqrt{\left\|\mathrm{Re}(s)^{1/2}\,\boldsymbol{e}_{\boldsymbol{\sigma}}\right\|^2_{\mathcal{T}_E,\mathbf{C}^{-1}}+\left\|\mathrm{Re}(s)^{1/2}\,\tau_E^{1/2}(\boldsymbol{e}_{\boldsymbol{u}}-\boldsymbol{e}_{\widehat{\boldsymbol{u}}})\right\|^2_{\partial\mathcal{T}_E}},$$

$$e_A:=\sqrt{\left\|\rho_f^{1/2}\mathrm{Re}(s)^{1/2}\,\boldsymbol{e}_{\boldsymbol{q}}\right\|^2_{\mathcal{T}_A}+\left\|\rho_f^{1/2}\mathrm{Re}(s)^{1/2}\,\tau_A^{1/2}(e_v-e_{\widehat{v}})\right\|^2_{\partial\mathcal{T}_A}}.$$

Let us now decompose now $\boldsymbol{e}_{\boldsymbol{\gamma}}=\boldsymbol{e}_{\boldsymbol{\gamma}}^0+\boldsymbol{e}_{\boldsymbol{\gamma}}^c$, where $\boldsymbol{e}_{\boldsymbol{\gamma}}^c$ is such that $\boldsymbol{e}_{\boldsymbol{\gamma}}^c|_K=\dfrac{1}{|K|}\displaystyle\int_K \boldsymbol{e}_{\boldsymbol{\gamma}}$ for all $K\in\mathcal{T}_E$ and $\boldsymbol{e}_{\boldsymbol{\gamma}}^0:=\boldsymbol{e}_{\boldsymbol{\gamma}}-\boldsymbol{e}_{\boldsymbol{\gamma}}^c$. Since $\boldsymbol{\delta}_{\boldsymbol{\sigma}}$ is orthogonal to piecewise constant polynomials, we have

$$(\boldsymbol{e}_{\boldsymbol{\gamma}},\boldsymbol{\delta}_{\boldsymbol{\sigma}})_{\mathcal{T}_E}=(\boldsymbol{e}_{\boldsymbol{\gamma}}^0,\boldsymbol{\delta}_{\boldsymbol{\sigma}})_{\mathcal{T}_E}+(\boldsymbol{e}_{\boldsymbol{\gamma}}^c,\boldsymbol{\delta}_{\boldsymbol{\sigma}})_{\mathcal{T}_E}=(\boldsymbol{e}_{\boldsymbol{\gamma}}^0,\boldsymbol{\delta}_{\boldsymbol{\sigma}})_{\mathcal{T}_E}.$$

Then, using this information and applying the triangle, Cauchy-Schwarz and Young inequalities several times to the expression (13), we deduce that there exists a positive constant C_1, independent of h, such that

$$e_E^2+e_A^2+\rho_E|s|^2\mathrm{Re}(s)\,\|\boldsymbol{e}_{\boldsymbol{u}}\|^2_{\mathcal{T}_E}+\frac{\rho_f}{c^2}|s|^2\mathrm{Re}(s)\,\|e_v\|^2_{\mathcal{T}_A}\le C_1\Theta(\boldsymbol{\sigma},\boldsymbol{u},\boldsymbol{\gamma},\boldsymbol{q},v)^2+\frac{1}{2}\|\boldsymbol{e}_{\boldsymbol{\gamma}}^0\|^2_{\mathcal{T}_E}. \tag{14}$$

5.3 Error estimates for the rotation.

It remains to obtain error bounds for $\boldsymbol{e}_{\boldsymbol{\gamma}}^0$ and $\boldsymbol{e}_{\boldsymbol{\gamma}}^c$. For the elasticity boundary value problem, these bounds were obtained in [20]. In our case, we obtain an optimal error estimate for $\|\boldsymbol{e}_{\boldsymbol{\gamma}}^0\|_{\mathcal{T}_E}$ following the same arguments presented in [20]. However, the error estimate for the L^2-norm of $\boldsymbol{e}_{\boldsymbol{\gamma}}^c$ depends on the term $\boldsymbol{e}_{\widehat{\boldsymbol{u}}}$ associated with the transmission conditions in Γ as we will see in the next result.

Lemma 5.3. *There exist positive constants, C_γ^c and C_γ^0, independent of h, such that*

$$\|\boldsymbol{e}_{\boldsymbol{\gamma}}^0\|_{\mathcal{T}_E} \le C_\gamma^0 \Theta(\boldsymbol{\sigma}, \boldsymbol{u}, \boldsymbol{\gamma}, \boldsymbol{q}, v). \tag{15a}$$

and

$$\|\boldsymbol{e}_{\boldsymbol{\gamma}}^c\|_{\mathcal{T}_E} \le C_\gamma^c \left(h^{-1/2} \Theta(\boldsymbol{\sigma}, \boldsymbol{u}, \boldsymbol{\gamma}, \boldsymbol{q}, v) + \|h^{-1} \boldsymbol{e}_{\boldsymbol{u}}\|_{\mathcal{T}_A} \right). \tag{15b}$$

Proof. By [20, Theorem 3.6], we now that

$$\|\boldsymbol{e}_{\boldsymbol{\gamma}}^0\|_{\mathcal{T}_E} \le \|\boldsymbol{e}_{\boldsymbol{\sigma}}\|_{\mathcal{T}_E} + ||\boldsymbol{\delta}_{\boldsymbol{\sigma}}||_{\mathcal{T}_E} + \|\boldsymbol{\delta}_{\boldsymbol{\gamma}}\|_{\mathcal{T}_E}.$$

The first term can be bounded by (14), and therefore

$$\|\boldsymbol{e}_{\boldsymbol{\gamma}}^0\|_{\mathcal{T}_E}^2 \lesssim \Theta(\boldsymbol{\sigma}, \boldsymbol{u}, \boldsymbol{\gamma}, \boldsymbol{q}, v)^2 + \frac{s^2}{2}\|\boldsymbol{\delta}_{\boldsymbol{\sigma}}\|_{\mathcal{T}_E}^2 + \frac{1}{2}\|\boldsymbol{e}_{\boldsymbol{\gamma}}^0\|_{\mathcal{T}_E}^2 + ||\boldsymbol{\delta}_{\boldsymbol{\sigma}}||_{\mathcal{T}_E}^2 + \|\boldsymbol{\delta}_{\boldsymbol{\gamma}}\|_{\mathcal{T}_E}^2 \lesssim \Theta(\boldsymbol{\sigma}, \boldsymbol{u}, \boldsymbol{\gamma}, \boldsymbol{q}, v)^2 + \frac{1}{2}\|\boldsymbol{e}_{\boldsymbol{\gamma}}^0\|_{\mathcal{T}_E}^2$$

and (15a) follows.

Now, we will modify the proof of [20, Theorem 3.8] to estimate $\boldsymbol{e}_{\boldsymbol{\gamma}}^c$. Let $\boldsymbol{\eta} := \boldsymbol{e}_{\boldsymbol{\gamma}}^c \in \underline{\boldsymbol{A}}_h^c$. There exists $\boldsymbol{v} \in \underline{\boldsymbol{H}}(\mathrm{div};\Omega_E) \cap \underline{\boldsymbol{\mathcal{P}}}_1(\mathcal{T}_E)$ satisfying the properties in (7). Then, taking $\boldsymbol{\tau} = \boldsymbol{v}$ in (12a) and using the fact that $\nabla\cdot \boldsymbol{v} = 0$, we obtain

$$(\mathbf{C}^{-1}\boldsymbol{e}_{\boldsymbol{\sigma}}, \boldsymbol{v})_{\mathcal{T}_E} + (\boldsymbol{e}_{\boldsymbol{\gamma}}, \boldsymbol{v})_{\mathcal{T}_E} - \langle \boldsymbol{e}_{\widehat{\boldsymbol{u}}}, \boldsymbol{v}\boldsymbol{n}\rangle_{\partial\mathcal{T}_E} = -(\mathbf{C}^{-1}\boldsymbol{\delta}_{\boldsymbol{\sigma}}, \boldsymbol{v})_{\mathcal{T}_E} - (\boldsymbol{\delta}_{\boldsymbol{\gamma}}, \boldsymbol{v})_{\mathcal{T}_E}.$$

Now, since $(\boldsymbol{e}_{\boldsymbol{\gamma}}, \boldsymbol{v})_{\mathcal{T}_E} = (\boldsymbol{e}_{\boldsymbol{\gamma}}^0, \boldsymbol{v})_{\mathcal{T}_E} + (\boldsymbol{e}_{\boldsymbol{\gamma}}^c, \boldsymbol{v})_{\mathcal{T}_E}$ and $(\boldsymbol{e}_{\boldsymbol{\gamma}}^c, \boldsymbol{v})_{\mathcal{T}_E} = \|\boldsymbol{e}_{\boldsymbol{\gamma}}^c\|_{\mathcal{T}_E}^2$, according to the second property in (7), we deduce that

$$\begin{aligned}\|\boldsymbol{e}_{\boldsymbol{\gamma}}^c\|_{\mathcal{T}_E}^2 =& -(\mathbf{C}^{-1}\boldsymbol{e}_{\boldsymbol{\sigma}}, \boldsymbol{v})_{\mathcal{T}_E} - (\boldsymbol{e}_{\boldsymbol{\gamma}}^0, \boldsymbol{v})_{\mathcal{T}_E} - (\mathbf{C}^{-1}\boldsymbol{\delta}_{\boldsymbol{\sigma}}, \boldsymbol{v})_{\mathcal{T}_E} - (\boldsymbol{\delta}_{\boldsymbol{\gamma}}, \boldsymbol{v})_{\mathcal{T}_E} + \langle \boldsymbol{e}_{\widehat{\boldsymbol{u}}}, \boldsymbol{v}\boldsymbol{n}\rangle_{\partial\mathcal{T}_E}\\ \lesssim& \,\Theta(\boldsymbol{\sigma}, \boldsymbol{u}, \boldsymbol{\gamma}, \boldsymbol{q}, v)\|\boldsymbol{e}_{\boldsymbol{\gamma}}^c\|_{\mathcal{T}_E} + |\langle \boldsymbol{e}_{\widehat{\boldsymbol{u}}}, \boldsymbol{v}\boldsymbol{n}\rangle_{\partial\mathcal{T}_E}|,\end{aligned}$$

where we have used the second and third properties of (7), and also the estimates (14) and (15a). For the last term, we have $\langle \boldsymbol{e}_{\widehat{\boldsymbol{u}}}, \boldsymbol{v}\boldsymbol{n}\rangle_{\partial\mathcal{T}_E} = \langle \boldsymbol{e}_{\widehat{\boldsymbol{u}}}, \boldsymbol{v}\boldsymbol{n}\rangle_{\Gamma}$ because $\boldsymbol{e}_{\widehat{\boldsymbol{u}}}$ is single-valued and $\boldsymbol{v} \in \boldsymbol{H}(\mathrm{div};\Omega_E)$, and this is precisely the term that in our case does not vanish, in contrast to the case in [20].

Let e be a face in Γ of an element $K \in \mathcal{T}_E$. By the discrete trace inequality, (14) and (7) we deduce that

$$\begin{aligned}\langle \boldsymbol{e}_{\widehat{\boldsymbol{u}}}, \boldsymbol{v}\boldsymbol{n}\rangle_e \le& \,\langle \tau_E^{1/2}(\boldsymbol{e}_{\widehat{\boldsymbol{u}}} - \boldsymbol{e}_{\boldsymbol{u}}), \tau_E^{-1/2}\boldsymbol{v}\boldsymbol{n}\rangle_e + \langle \boldsymbol{e}_{\boldsymbol{u}}, \boldsymbol{v}\boldsymbol{n}\rangle_e\\ \lesssim& \,h^{-1/2}\Theta(\boldsymbol{\sigma}, \boldsymbol{u}, \boldsymbol{\gamma}, \boldsymbol{q}, v)\|\boldsymbol{e}_{\boldsymbol{\gamma}}^c\|_K + \|h^{-1}\boldsymbol{e}_{\boldsymbol{u}}\|_K\|\boldsymbol{e}_{\boldsymbol{\gamma}}^c\|_K,\end{aligned}$$

which implies (15b). ☐

If we consider the energy error estimate (14) to bound $\|\boldsymbol{e}_{\boldsymbol{u}}\|_{\mathcal{T}_E}$, we will obtain the suboptimal error bound

$$\|\boldsymbol{e}_{\boldsymbol{\gamma}}^c\|_{\mathcal{T}_E} \lesssim h^{-1}\Theta(\boldsymbol{\sigma}, \boldsymbol{u}, \boldsymbol{\gamma}, \boldsymbol{q}, v).$$

We can improve this result by considering a duality argument and gain an additional factor of $h^{1/2}$. In addition, the energy estimate (13) provides an order of convergence of h^{k+1} for the projection errors $\boldsymbol{e}_{\boldsymbol{u}}$ and e_v. Using also a duality argument, it is possible to prove the superconvergence for $\boldsymbol{e}_{\boldsymbol{u}}$ and e_v, as we will show in the next section.

5.4 The duality argument.

Given $\boldsymbol{\theta_e} \in \boldsymbol{L}^2(\Omega_E)$ and $\theta_a \in L^2(\Omega_A)$, we introduce the following auxiliary problem:

$$\begin{aligned}
\mathbf{C}^{-1}\boldsymbol{\psi_e} - \nabla\boldsymbol{\phi_e} + \boldsymbol{\xi_e} &= \mathbf{0} && \text{in } \Omega_E,\\
\nabla\cdot\boldsymbol{\psi_e} - \rho_E\overline{s^2}\,\boldsymbol{\phi_e} &= \boldsymbol{\theta_e} && \text{in } \Omega_E,\\
\boldsymbol{\xi_a} + \nabla\phi_a &= \mathbf{0} && \text{in } \Omega_A,\\
\nabla\cdot\boldsymbol{\xi_a} - \overline{(s/c)^2}\,\phi_a &= \theta_a && \text{in } \Omega_A,\\
\boldsymbol{\xi_a}\cdot\boldsymbol{n}_A + \overline{s}\,\boldsymbol{\phi_e}\cdot\boldsymbol{n}_E &= 0 && \text{on } \Gamma,\\
\boldsymbol{\psi_e}\boldsymbol{n}_E + \rho_f\overline{s}\,\phi_a\,\boldsymbol{n}_A &= 0 && \text{on } \Gamma,\\
\phi_a &= 0 && \text{on } \Gamma_A^D,\\
\boldsymbol{\xi_a}\cdot\boldsymbol{n}_A &= 0 && \text{on } \Gamma_A^N.
\end{aligned}$$

Here, $\boldsymbol{\xi_e} = \frac{1}{2}(\nabla\boldsymbol{\phi_e} - \nabla^\top\boldsymbol{\phi_e})$. We assume that this problem admits the regularity estimate

$$\|\boldsymbol{\psi_e}\|_{\underline{\boldsymbol{H}}^{s_e}(\Omega_E)} + \|\boldsymbol{\phi_e}\|_{\boldsymbol{H}^{1+s_e}(\Omega_E)} + \|\boldsymbol{\xi_a}\|_{\boldsymbol{H}^{s_a}(\Omega_A)} + \|\phi_a\|_{H^{1+s_a}(\Omega_A)} \lesssim \|\boldsymbol{\theta_e}\|_{\Omega_E} + \|\theta_a\|_{\Omega_A} \tag{16}$$

for some $s_e, s_a \geq 0$.

Performing calculations analogous to those in [18, 20], it is possible to obtain the following lemma:

Lemma 5.4. *For any $\boldsymbol{\phi_e^k} \in \boldsymbol{\mathcal{P}}_k(\mathcal{T}_E)\,, \boldsymbol{\phi_e^{k-1}} \in \boldsymbol{\mathcal{P}}_{k-1}(\mathcal{T}_E)$ and $\boldsymbol{\theta_e} \in \boldsymbol{L}^2(\Omega_E)$, we have*

$$\begin{aligned}
(\boldsymbol{e_u}, \boldsymbol{\theta_e})_{\mathcal{T}_E} = {} & (\mathbf{C}^{-1}\boldsymbol{e_\sigma}, \boldsymbol{\delta_{\psi_e}})_{\mathcal{T}_E} + (\boldsymbol{e_\gamma}, \boldsymbol{\delta_{\psi_e}})_{\mathcal{T}_E} + (\boldsymbol{e_\sigma}, \boldsymbol{\delta_{\xi_e}})_{\mathcal{T}_E}\\
& + (\boldsymbol{\delta_\sigma}, \boldsymbol{\delta_{\xi_e}})_{\mathcal{T}_E} + (\mathbf{C}^{-1}\boldsymbol{\delta_\sigma}, \boldsymbol{\delta_{\psi_e}})_{\mathcal{T}_E} + (\boldsymbol{\delta_\gamma}, \boldsymbol{\delta_{\psi_e}})_{\mathcal{T}_E} - (\boldsymbol{\delta_\sigma}, \nabla(\boldsymbol{\phi_e} - \boldsymbol{\phi_e^k}))_{\mathcal{T}_E}\\
& - \rho_E s^2(\boldsymbol{u} - \boldsymbol{u}_h, \boldsymbol{\delta_{\phi_e}})_{\mathcal{T}_E} + \rho_E s^2(\boldsymbol{\delta_u}, \boldsymbol{\phi_e} - \boldsymbol{\phi_e^{k-1}})_{\mathcal{T}_E} + \langle \boldsymbol{e_{\widehat{u}}}, \boldsymbol{\psi_e}\boldsymbol{n}_E\rangle_\Gamma - \langle \boldsymbol{e_{\widehat{\sigma}}}\boldsymbol{n}_E, \boldsymbol{\phi_e}\rangle_\Gamma.
\end{aligned} \tag{17a}$$

In addition, for any $\phi_a^k \in \mathcal{P}_k(\mathcal{T}_A)\,, \phi_a^{k-1} \in \mathcal{P}_{k-1}(\mathcal{T}_A)$ and $\theta_a \in L^2(\Omega_A)$, there holds

$$\begin{aligned}
(e_v, \theta_a)_{\mathcal{T}_A} = {} & (\boldsymbol{q} - \boldsymbol{q}_h, \boldsymbol{\delta_{\xi_a}})_{\mathcal{T}_A} - (\boldsymbol{\delta_q}, \nabla(\phi_a - \phi_a^k))_{\mathcal{T}_A} - \langle \boldsymbol{e_{\widehat{q}}}\cdot\boldsymbol{n}_A, \phi_a\rangle_\Gamma\\
& - (s/c)^2(v - v_h, \delta_{\phi_a})_{\mathcal{T}_A} + (s/c)^2(\delta_v, \phi_a - \phi_a^{k-1})_{\mathcal{T}_A} + \langle e_{\widehat{v}}, \boldsymbol{\xi_a}\cdot\boldsymbol{n}_A\rangle_\Gamma.
\end{aligned} \tag{17b}$$

Based on the above two lemmas, we can derive the estimate.

Corollary 5.4.1. *If the regularity assumption (16) holds with $s_e, s_a \geq 0$ and $k \geq 1$, then*

$$\|e_v\|_{\mathcal{T}_A} + \|\boldsymbol{e_u}\|_{\mathcal{T}_E} \lesssim (h^{s_e} + h^{s_a})\Theta(\boldsymbol{\sigma}, \boldsymbol{u}, \boldsymbol{\gamma}, \boldsymbol{q}, v), \tag{18a}$$

$$\|\boldsymbol{e_\gamma^c}\|_{\mathcal{T}_E} \lesssim (h^{-1/2} + h^{s_e-1} + h^{s_a-1})\Theta(\boldsymbol{\sigma}, \boldsymbol{u}, \boldsymbol{\gamma}, \boldsymbol{q}, v). \tag{18b}$$

Proof. Taking $\boldsymbol{\theta_e} = \boldsymbol{e_u}$ in (17a) and $\theta_a = e_v$ in (17b), let us add $\|e_v\|^2_{\mathcal{T}_A}$ and $\rho_f^{-1}\|\boldsymbol{e_u}\|^2_{\mathcal{T}_E}$. Then, by (12k) and (12l), the terms in Γ cancel out and we obtain

$$\begin{aligned}
\|e_v\|^2_{\mathcal{T}_A} + \rho_f\|\boldsymbol{e_u}\|^2_{\mathcal{T}_E} = {} & (\boldsymbol{q} - \boldsymbol{q}_h, \boldsymbol{\delta_{\xi_a}})_{\mathcal{T}_A} - (\boldsymbol{\delta_q}, \nabla(\phi_a - \phi_a^k))_{\mathcal{T}_A} - (s/c)^2(v - v_h, \delta_{\phi_a})_{\mathcal{T}_A}\\
& + (s/c)^2(\delta_v, \phi_a - \phi_a^{k-1})_{\mathcal{T}_A} + \rho_f^{-1}\big\{(\mathbf{C}^{-1}\boldsymbol{e_\sigma}, \boldsymbol{\delta_{\psi_e}})_{\mathcal{T}_E} + (\boldsymbol{e_\gamma}, \boldsymbol{\delta_{\psi_e}})_{\mathcal{T}_E}\\
& + (\boldsymbol{e_\sigma}, \boldsymbol{\delta_{\xi_e}})_{\mathcal{T}_E} + (\boldsymbol{\delta_\sigma}, \boldsymbol{\delta_{\xi_e}})_{\mathcal{T}_E} + (\mathbf{C}^{-1}\boldsymbol{\delta_\sigma}, \boldsymbol{\delta_{\psi_e}})_{\mathcal{T}_E} + (\boldsymbol{\delta_\gamma}, \boldsymbol{\delta_{\psi_e}})_{\mathcal{T}_E}\\
& - (\boldsymbol{\delta_\sigma}, \nabla(\boldsymbol{\phi_e} - \boldsymbol{\phi_e^k}))_{\mathcal{T}_E} - \rho_E s^2(\boldsymbol{u} - \boldsymbol{u}_h, \boldsymbol{\delta_{\phi_e}})_{\mathcal{T}_E} + \rho_E s^2(\boldsymbol{\delta_u}, \boldsymbol{\phi_e} - \boldsymbol{\phi_e^{k-1}})_{\mathcal{T}_E}\big\}
\end{aligned}$$

Now, we notice that

$$(\boldsymbol{e_\gamma}, \boldsymbol{\delta_{\psi_e}})_{\mathcal{T}_E} = (\boldsymbol{e_\gamma^0}, \boldsymbol{\delta_{\psi_e}})_{\mathcal{T}_E} + (\boldsymbol{e_\gamma^c}, \boldsymbol{\delta_{\psi_e}})_{\mathcal{T}_E} = (\boldsymbol{e_\gamma^0}, \boldsymbol{\delta_{\psi_e}})_{\mathcal{T}_E},$$

because $\boldsymbol{\delta_{\psi_e}}$ is orthogonal to piecewise constant polynomials. In addition, the terms on Γ cancel each other out. Then, applying the triangular and Cauchy-Schwarz inequalities, we obtain

$$\|e_v\|^2_{\mathcal{T}_A} + \rho_f\|\boldsymbol{e_u}\|^2_{\mathcal{T}_E} \lesssim (OPT \times APT) + \|\boldsymbol{\delta_{\psi_e}}\|_{\mathcal{T}_E}\|\boldsymbol{e_\gamma^0}\|_{\mathcal{T}_E}, \tag{19}$$

where OPT stands for "original problem terms" and APT for "auxiliary problem terms":

$$OPT := \Big(\|\boldsymbol{q}-\boldsymbol{q}_h\|^2_{\mathcal{T}_A} + \|v-v_h\|^2_{\mathcal{T}_A} + \|\boldsymbol{u}-\boldsymbol{u}_h\|^2_{\mathcal{T}_E} + \|\boldsymbol{e_\sigma}\|^2_{\mathcal{T}_E} + \|\boldsymbol{\delta_q}\|^2_{\mathcal{T}_A} + \|\delta_v\|^2_{\mathcal{T}_A} + \|\boldsymbol{\delta_\sigma}\|^2_{\mathcal{T}_E} + \|\boldsymbol{\delta_u}\|^2_{\mathcal{T}_E} + \|\boldsymbol{\delta_\gamma}\|^2_{\mathcal{T}_E} \Big)^{1/2}$$

and

$$APT := \Big(\|\boldsymbol{\delta_{\xi_a}}\|^2_{\mathcal{T}_A} + \|\delta_{\phi_a}\|^2_{\mathcal{T}_A} + \left\|\nabla(\phi_a-\phi_a^k)\right\|^2_{\mathcal{T}_A} + \left\|\phi_a-\phi_a^{k-1}\right\|^2_{\mathcal{T}_A} + \|\boldsymbol{\delta_{\xi_e}}\|^2_{\mathcal{T}_E} + \|\boldsymbol{\delta_{\phi_e}}\|^2_{\mathcal{T}_E} + \left\|\nabla(\boldsymbol{\phi_e}-\boldsymbol{\phi_e^k})\right\|^2_{\mathcal{T}_E} + \left\|\boldsymbol{\phi_e}-\boldsymbol{\phi_e^{k-1}}\right\|^2_{\mathcal{T}_E} \Big)^{1/2}.$$

In the OPT term, we add and subtract the projections $\boldsymbol{\Pi_A q}$, $\Pi_A v$ and $\boldsymbol{\Pi_E u}$ in the first three terms, use (14) and the definition of $\Theta(\boldsymbol{\sigma},\boldsymbol{u},\boldsymbol{\gamma},\boldsymbol{q},v)$, to conclude that

$$OPT \lesssim \Theta(\boldsymbol{\sigma},\boldsymbol{u},\boldsymbol{\gamma},\boldsymbol{q},v) + \sqrt{\frac{1}{2}}\|\boldsymbol{e}^0_{\boldsymbol{\gamma}}\|_{\mathcal{T}_E}.$$

Regarding the APT, we first consider ϕ_a^{k-1} and ϕ_a^k as the L^2-projections of ϕ_a over $\mathcal{P}_{k-1}(\mathcal{T}_A)$ and $\mathcal{P}_k(\mathcal{T}_A)$, resp. Similarly, we take $\boldsymbol{\phi_e^{k-1}}$ and $\boldsymbol{\phi_e^k}$ as the L^2-projections of $\boldsymbol{\phi_e}$ over $\boldsymbol{\mathcal{P}}_{k-1}(\mathcal{T}_E)$ and $\boldsymbol{\mathcal{P}}_k(\mathcal{T}_E)$, resp. Then, by the approximation properties of the L^2- [22, Lemma 1.58] and the HDG-projections (10)-(11), and assuming the regularity assumption (16), we can deduce that

$$APT \lesssim (h^{s_e}+h^{s_a})\left(\|e_v\|_{\mathcal{T}_A} + \sqrt{\rho_f}\,\|\boldsymbol{e_u}\|_{\mathcal{T}_E}\right).$$

Then, replacing these expressions in (19), and noticing that

$$\|\boldsymbol{\delta_{\psi_e}}\|_{\mathcal{T}_E} \lesssim h(\|\boldsymbol{\theta_e}\|_{\Omega_E} + \|\theta_a\|_{\Omega_A}) \lesssim h\left(\|e_v\|_{\mathcal{T}_A} + \sqrt{\rho_f}\,\|\boldsymbol{e_u}\|_{\mathcal{T}_E}\right),$$

we obtain that

$$\begin{aligned}\|e_v\|^2_{\mathcal{T}_A} + \rho_f\,\|\boldsymbol{e_u}\|^2_{\mathcal{T}_E} &\lesssim \left(\Theta(\boldsymbol{\sigma},\boldsymbol{u},\boldsymbol{\gamma},\boldsymbol{q},v) + \sqrt{\frac{1}{2}}\|\boldsymbol{e}^0_{\boldsymbol{\gamma}}\|_{\mathcal{T}_E}\right)\left((h^{s_e}+h^{s_a})\left(\|e_v\|_{\mathcal{T}_A} + \sqrt{\rho_f}\,\|\boldsymbol{e_u}\|_{\mathcal{T}_E}\right)\right) \\ &\quad + \|\boldsymbol{\delta_{\psi_e}}\|_{\mathcal{T}_E}\|\boldsymbol{e}^0_{\boldsymbol{\gamma}}\|_{\mathcal{T}_E} \\ &\lesssim \left(\Theta(\boldsymbol{\sigma},\boldsymbol{u},\boldsymbol{\gamma},\boldsymbol{q},v) + \|\boldsymbol{e}^0_{\boldsymbol{\gamma}}\|_{\mathcal{T}_E}\right)\left((h^{s_e}+h^{s_a})\left(\|e_v\|_{\mathcal{T}_A} + \sqrt{\rho_f}\,\|\boldsymbol{e_u}\|_{\mathcal{T}_E}\right)\right),\end{aligned}$$

which implies that

$$\|e_v\|^2_{\mathcal{T}_A} + \rho_f\,\|\boldsymbol{e_u}\|^2_{\mathcal{T}_E} \lesssim (h^{s_e}+h^{s_a})\,\left(\Theta(\boldsymbol{\sigma},\boldsymbol{u},\boldsymbol{\gamma},\boldsymbol{q},v) + \|\boldsymbol{e}^0_{\boldsymbol{\gamma}}\|_{\mathcal{T}_E}\right) \lesssim\, (h^{s_e}+h^{s_a})\,\Theta(\boldsymbol{\sigma},\boldsymbol{u},\boldsymbol{\gamma},\boldsymbol{q},v),$$

□

Summarizing all previous estimates, and using the estimate in Lemma 5.1, we have the following result.

Theorem 5.5. *If* $(\boldsymbol{\sigma},\boldsymbol{u},\boldsymbol{\gamma},\boldsymbol{q},v) \in \underline{\boldsymbol{H}}^{k+1}(\Omega_E)\times\boldsymbol{H}^{k+1}(\Omega_E)\times\underline{\boldsymbol{H}}^{k+1}(\Omega_E)\times\boldsymbol{H}^{k+1}(\Omega_A)\times H^{k+1}(\Omega_A)$ *and* $k\geq 1$, *then*

$$||\boldsymbol{\sigma}-\boldsymbol{\sigma}_h||_{\mathcal{T}_E} + ||\boldsymbol{u}-\boldsymbol{u}_h||_{\mathcal{T}_E} + ||\boldsymbol{q}-\boldsymbol{q}_h||_{\mathcal{T}_A} + ||v-v_h||_{\mathcal{T}_A} \lesssim h^{k+1}.$$

and

$$||\boldsymbol{\gamma}-\boldsymbol{\gamma}_h||_{\mathcal{T}_A} \lesssim h^k(h^{1/2}+h^{s_e}+h^{s_a}).$$

Finally, we have the following error estimates for the numerical traces:

Lemma 5.6. *Under the same hypothesis of previous theorem, there holds*

$$|||\boldsymbol{e}_{\widehat{\boldsymbol{u}}}|||_{\partial\mathcal{T}_E} \lesssim (h^{-1/2} + h^{s_e-1} + h^{s_a-1})h^{k+1} \tag{20a}$$

and

$$|||e_{\hat{v}}|||_{\partial\mathcal{T}_A} \lesssim (h + h^{s_e} + h^{s_a})h^{k+1}. \tag{20b}$$

where, for $\dagger \in \{A, E\}$*, we consider the norm*

$$|||\cdot|||_{\partial\mathcal{T}_\dagger} := \left(\sum_{K\in\mathcal{T}_\dagger} h_K \|\cdot\|^2_{\partial K}\right)^{1/2}.$$

Proof. By following the argument in the proof of Theorem 4.1 in [18], let $K \in \mathcal{T}_E$ and $\boldsymbol{\tau}_K \in \underline{\boldsymbol{\mathcal{P}}}_k(K)$ such that $\boldsymbol{\tau n} = \boldsymbol{e}_{\widehat{\boldsymbol{u}}}$ on ∂K and $\|\boldsymbol{\tau}_K\|_K \lesssim h_K^{1/2}\|\boldsymbol{e}_{\widehat{\boldsymbol{u}}}\|_{\partial K}$. According to (12a), taking $\boldsymbol{\tau} = \boldsymbol{\tau}_K$ in K and $\boldsymbol{\tau} = 0$ otherwise, we can write

$$\|\boldsymbol{e}_{\widehat{\boldsymbol{u}}}\|^2_{\partial K} = (\mathbf{C}^{-1}\boldsymbol{e}_{\boldsymbol{\sigma}}, \boldsymbol{\tau})_K + (\boldsymbol{e}_{\boldsymbol{u}}, \nabla\cdot\boldsymbol{\tau})_K + (\boldsymbol{e}_{\boldsymbol{\gamma}}, \boldsymbol{\tau})_K + (\mathbf{C}^{-1}\boldsymbol{\delta}_{\boldsymbol{\sigma}}, \boldsymbol{\tau})_K + (\boldsymbol{\delta}_{\boldsymbol{\gamma}}, \boldsymbol{\tau})_K.$$

By the Cauchy-Schwarz and inverse inequalities, we can obtain

$$\|\boldsymbol{e}_{\widehat{\boldsymbol{u}}}\|^2_{\partial K} \lesssim \left(\|\boldsymbol{e}_{\boldsymbol{\sigma}}\|_K + h_K^{-1}\|\boldsymbol{e}_{\boldsymbol{u}}\|_K + \|\boldsymbol{e}_{\boldsymbol{\gamma}}\|_K + \|\boldsymbol{\delta}_{\boldsymbol{\sigma}}\|_K + \|\boldsymbol{\delta}_{\boldsymbol{\gamma}}\|_K\right)\|\boldsymbol{\tau}\|_K,$$

which implies that

$$\|\boldsymbol{e}_{\widehat{\boldsymbol{u}}}\|_{\partial K} \lesssim h_K^{1/2}\|\boldsymbol{e}_{\boldsymbol{\sigma}}\|_K + h_K^{-1/2}\|\boldsymbol{e}_{\boldsymbol{u}}\|_K + h_K^{1/2}\|\boldsymbol{e}_{\boldsymbol{\gamma}}\|_K + h_K^{1/2}\|\boldsymbol{\delta}_{\boldsymbol{\sigma}}\|_K + h_K^{1/2}\|\boldsymbol{\delta}_{\boldsymbol{\gamma}}\|_K,$$

because $\|\boldsymbol{\tau}_K\|_K \lesssim h_K^{1/2}\|\boldsymbol{e}_{\widehat{\boldsymbol{u}}}\|_{\partial K}$. This expression, together with (18a) and (14) to bound $\|\boldsymbol{e}_{\boldsymbol{u}}\|_K$ and $\|\boldsymbol{e}_{\boldsymbol{\sigma}}\|_K$, respectively, implies that

$$\left(\sum_{K\in\mathcal{T}_E} h_K\|\boldsymbol{e}_{\widehat{\boldsymbol{u}}}\|^2_{\partial K}\right)^{1/2} \lesssim h\Theta(\boldsymbol{\sigma}, \boldsymbol{u}, \boldsymbol{\gamma}, \boldsymbol{q}, v) + \|\boldsymbol{e}_{\boldsymbol{\gamma}}\|_{\mathcal{T}_E}.$$

The estimate follows after using (15a) and (18b).

A similar procedure for $e_{\hat{v}}$ (see also the proof of Theorem 4.1 of [18]) leads to

$$h_K^{1/2}\|e_{\hat{v}}\|_{\partial K} \lesssim h_K\|\boldsymbol{e}_{\boldsymbol{q}}\|_K + \|e_v\|_K + h_K\|\boldsymbol{\delta}_{\boldsymbol{q}}\|_K,$$

for $K \in \mathcal{T}_A$. Adding over K,

$$\left(\sum_{K\in\mathcal{T}_A} h_K\|e_{\hat{v}}\|^2_{\partial K}\right)^{1/2} \lesssim (h + h^{s_e} + h^{s_a})\Theta(\boldsymbol{\sigma}, \boldsymbol{u}, \boldsymbol{\gamma}, \boldsymbol{q}, v),$$

where we used (14), (15a) and (18a). The result follows after considering the estimate in Lemma 5.1 □

6 Numerical Experiments

6.1 Acoustic problem.

To test our HDG scheme applied to the acoustic problem, we consider equations (1c)-(1d) complemented with Dirichlet boundary conditions $v = g_D$ on $\partial\Omega_A$. We take a manufactured acoustic field $v(x, y) = \sin(x)\sin(y)$. The source f and boundary data g_D are set in such a way that v satisfies (1c)-(1d) in a domain $\Omega_A = (0, 1)^2$, with $c = 1$ and, for example, $s = 2 - i$. The stabilization parameter τ_A is taken to be equal to one everywhere. As it can be inferred from Theorem 5.5 and (20a) (see also [18]), the theoretical orders of convergence for this case are h^{k+1} for v and $\boldsymbol{q}$; and h^{k+2} for the numerical trace, since the domain is convex ($s_a = 1$).

We consider quasi-uniform refinements of Ω_A and set $k \in \{1, 2, 3\}$ in the local spaces. Figure 2 shows the results obtained for this problem, where N is the number of mesh triangles. Note that for the errors in $\boldsymbol{q}$ and v the optimal theoretical order of convergence $k + 1$ was reached. In turn, for the numerical trace we can see an order of superconvergence $k + 2$, as expected.

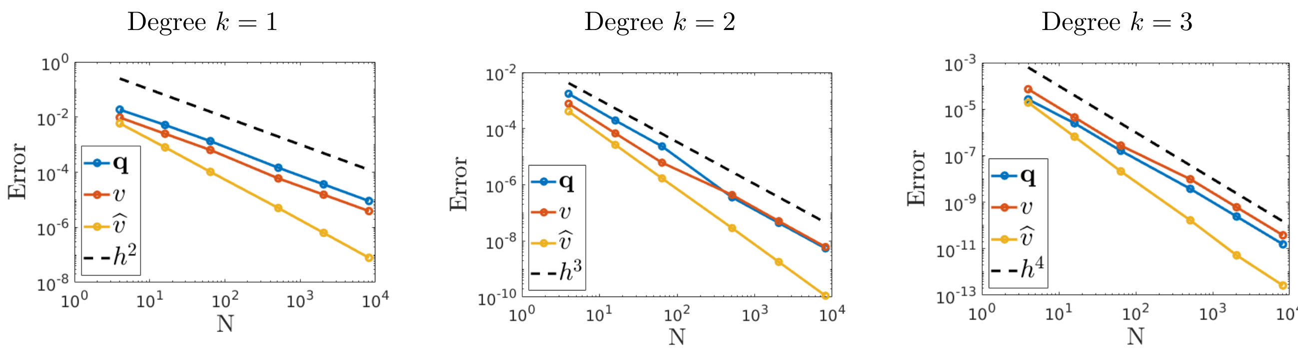

Figure 2: Discretization error as a function of the number of triangles in the domain for the acoustic problem.

6.2 Elastic problem.

Analogously to the previous subsection, let us apply the HDG scheme to the equations (1a)-(1b) considering $\Omega_E = (0,1)^2, \rho_E = 1, s = 2 - i$ and $\tau_E = 1$ everywhere. The source $\boldsymbol{f}$ and the Dirichlet boundary condition are defined such that

$$\boldsymbol{u}(x,y) = \begin{pmatrix} \sin(\pi x)\cos(\pi y) \\ \cos(\pi x)\sin(\pi y) \end{pmatrix}, \quad (x,y) \in (0,1)^2,$$

is the exact solution of the problem.

It is known that the Lamé's first parameter (λ) and the shear modulus (μ) (or Lamé's second parameter) satisfy the following expressions in terms of the Young's modulus (E) and the Poisson's ratio (ν):

$$\lambda = \frac{E\nu}{(1+\nu)(1-2\nu)} \qquad \text{and} \qquad \mu = \frac{E}{2(1+\nu)},$$

so let us take $E = 1$ and two values of ν, 0.3 and 0.49999 (a nearly incompressible isotropic material deformed elastically at small strains would have a Poisson's ratio of exactly 0.5).

From Theorem 5.5, we can deduce that the theoretical order of convergence is h^{k+1} for the displacements and the Cauchy stress tensor. Now, the negative powers of h in (15b) are due to the term $\langle \boldsymbol{e}_{\widehat{\boldsymbol{u}}}, v\boldsymbol{n}\rangle_{\partial\mathcal{T}_E}$ in the proof of Lemma 5.3. This term arises when coupling the elasticity and acoustic equations. Since in this example there is no coupling, the term $\langle \boldsymbol{e}_{\widehat{\boldsymbol{u}}}, v\boldsymbol{n}\rangle_{\partial\mathcal{T}_E}$ disappears and we can obtain that

$$\|\boldsymbol{e}^c_{\boldsymbol{\gamma}}\|_{\mathcal{T}_E} \lesssim \Theta(\boldsymbol{\sigma}, \boldsymbol{u}, \boldsymbol{\gamma}, \boldsymbol{q}, v).$$

Therefore, the theory guarantees an order h^{k+1} for the rotation, which agrees with the results in [20]. The same reason led the suboptimal estimates in (20a). Since in this example we are considering only the elasticity problem in a convex domain, we have regularity $s_e = 1$ and (20a) can be improved:

$$\|\!|\boldsymbol{e}_{\widehat{\boldsymbol{u}}}|\!\|_{\partial\mathcal{T}_E} \lesssim h^{k+2}.$$

Moreover, the HDG scheme is also optimal in the nearly incompressible case [7, 20].

The numerical results are shown in Figure 3. Observe that the experimental orders of convergence of the errors in $\boldsymbol{\sigma}, \boldsymbol{u}$ and $\boldsymbol{\gamma}$, $k+1$, coincide with the theoretical results. In addition, for the numerical trace of $\boldsymbol{u}$ we also have a superconvergence of order $k+2$.

6.3 Coupled problem.

We now test our HDG scheme applied to the coupled problem (1a)-(1h) with Dirichlet boundary conditions $v = g_D$ on Γ_A. We take a manufactured acoustic field $v(x,y) = \sin(x)\sin(y)$. The source f and boundary data g_D are set in such a way that v satisfies (1c)-(1d) in a domain $\Omega_A = (-2,2)^2$, with $c = 1$ and $s = 2 - i$. For the elastic region, we consider $\Omega_E = (-1,1)^2, \rho_E = 1$ and $\tau_E = 1$ everywhere. The source $\boldsymbol{f}$ is defined such that

$$\boldsymbol{u}(x,y) = \begin{pmatrix} \sin(\pi x)\cos(\pi y) \\ \cos(\pi x)\sin(\pi y) \end{pmatrix}, \quad (x,y) \in (-1,1)^2,$$

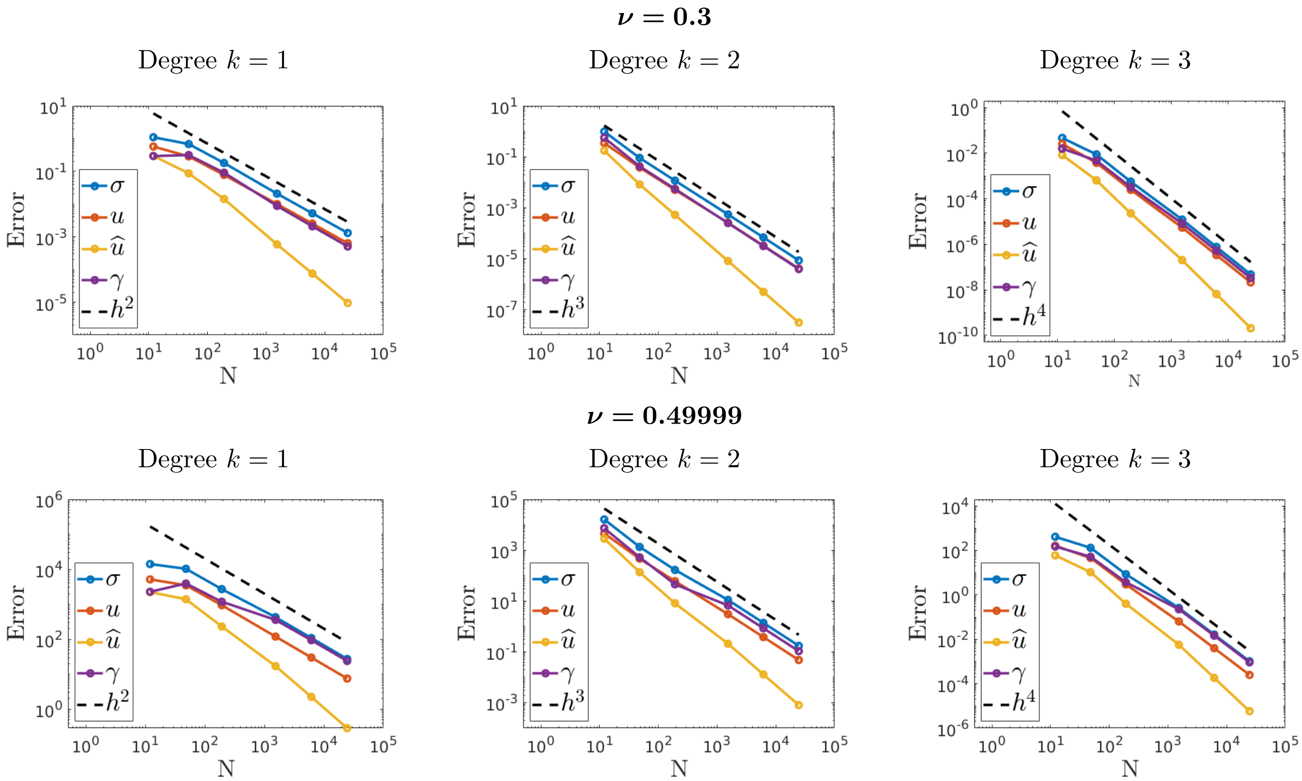

Figure 3: Discretization error as a function of the number of elements in the elastic domain for Poisson's ratio $\nu = 0.3$ (first row) and $\nu = 0.49999$ (second row).

satisfies (1a)-(1b). We set the field $v^{\text{inc}}(x, y) = -\sin(x)\sin(y)$ and include additional terms on the right-hand sides of (1e)-(1f) so that our manufactured solution satisfies them.

Figure 4 presents the numerical results obtained. The experimental orders of convergence of $\boldsymbol{\sigma}$, $\boldsymbol{u}$, $\boldsymbol{q}$ and v coincide with the theoretical results predicted by Theorem 5.5. Now, for the rotation, Theorem 5.5 guarantees an order $h^{k+\min\{1/2, s_e, s_1\}}$, where we recall that s_e and s_a are the regularity indices in (16). Numerically, we observe a better result and obtain a convergence rate of h^{k+1}. Moreover, Theorem 5.6 predicts $|||\boldsymbol{e}_{\widehat{\boldsymbol{u}}}|||_{\partial\mathcal{T}_E} \lesssim h^{k+\min\{1/2, s_e, s_a\}}$ and $|||e_{\hat{v}}|||_{\partial\mathcal{T}_A} \lesssim h^{k+1+\min\{1, s_e, s_a\}}$. Computationally superconvergence of order $k+2$ is observed for the numerical traces.

7 Concluding remarks

The current work presents what—to the authors's best knowledge—is the first analysis and proof of convergence of an HDG discretization for the a Laplace–domain system modeling the interaction between acoustic and elastic waves on a bounded domain. The numerical experiments suggest that convergence rates superior to those theoretically obtained can be expected. The challenge of rigorously establishing such improved rates remains outstanding.

In practical applications, it is often the case that the domain of interest is unbounded. The work presented here is a first step towards a discretization of such physically meaningful cases. In particular, the treatment of the coupling between the scheme analyzed in this communication with a boundary integral formulation for the exterior problem is the subject of ongoing work.

Acknowledgments

Fernando Artaza-Covarrubias was partially funded by ANID-Chile through the grant Fondecyt Regular 1240183. Tonatiuh Sánchez-Vizuet was partially funded by the U. S. National Science Foundation through the grant NSF-DMS-2137305. Manuel Solano was partially funded by ANID-Chile through the grants Fondecyt Regular 1240183

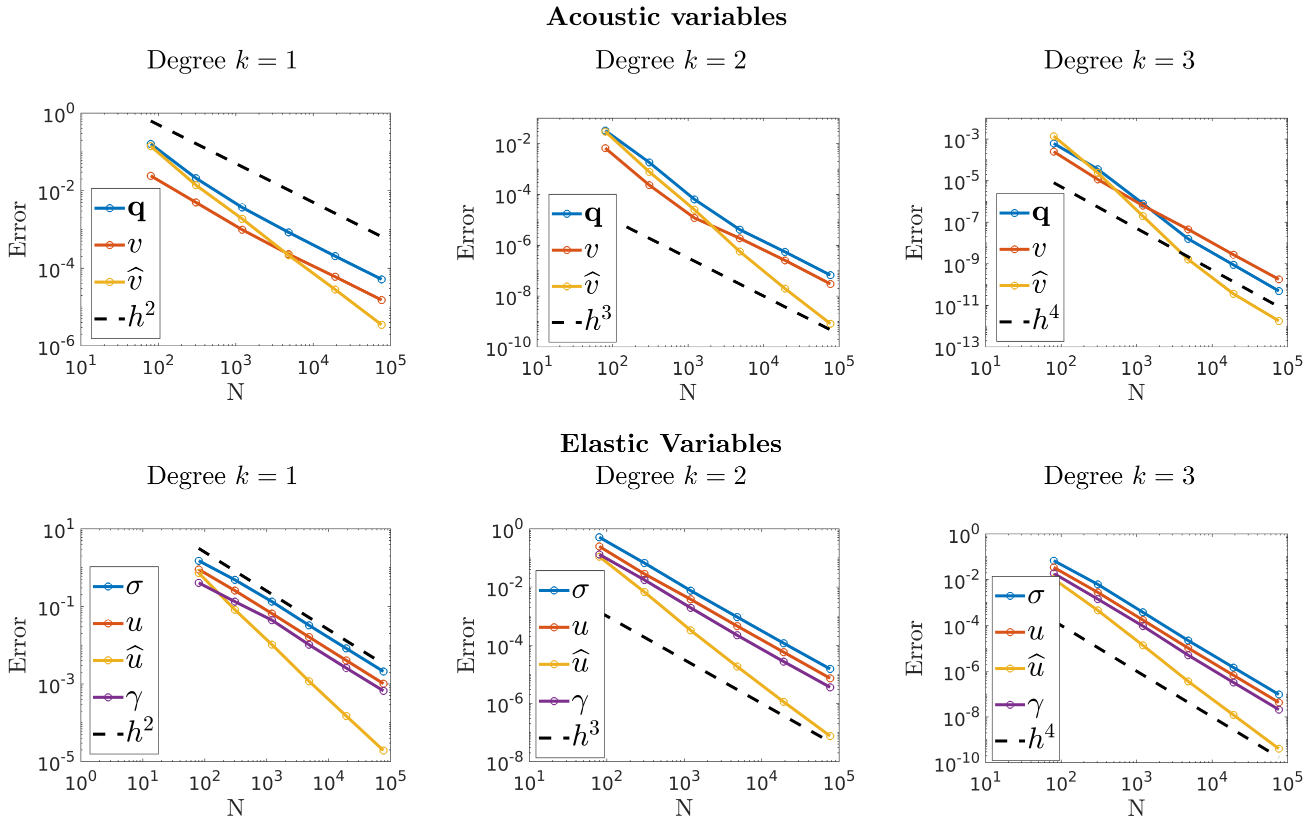

Figure 4: Discretization error as a function of the number of elements in the domain for the coupled acoustic/elastic problem. Acoustic variables are displayed on the first column and elastic variables on the second column.

and Basal FB210005.

References

[1] C. J. S. Alves and P. R. S. Antunes. Wave scattering problems in exterior domains with the method of fundamental solutions. *Numerische Mathematik*, 156(2):375–394, Feb. 2024.

[2] R. Araya, R. Rodríguez, and P. Venegas. Numerical analysis of a time domain elastoacoustic problem. *IMA Journal of Numerical Analysis*, 40(2):1122–1153, 01 2019.

[3] I. Bermúdez, J. Manríquez, and M. Solano. A hybridizable discontinuous Galerkin method for Stokes/Darcy coupling on dissimilar meshes. *IMA J. Numer. Anal.*, 2025.

[4] T. S. Brown, T. Sánchez-Vizuet, and F.-J. Sayas. Evolution of a semidiscrete system modeling the scattering of acoustic waves by a piezoelectric solid. *ESAIM: Mathematical Modelling and Numerical Analysis (M2AN)*, 52(2):423–455, Mar. 2018.

[5] R. Bustinza, B. López-Rodríguez, and M. Osorio. An a priori error analysis of an HDG method for an eddy current problem. *Mathematical Methods in the Applied Sciences*, 41(7):2795–2810, 2018.

[6] L. Camargo, B. López-Rodríguez, M. Osorio, and M. Solano. An HDG method for Maxwell's equations in heterogeneous media. *Computer Methods in Applied Mechanics and Engineering*, 368:113178, 2020.

[7] J. M. Cárdenas and M. Solano. A high order unfitted hybridizable discontinuous Galerkin method for linear elasticity. *IMA Journal of Numerical Analysis*, 44(2):945–979, 05 2023.

[8] A. Cesmelioglu, B. Cockburn, N. C. Nguyen, and J. Peraire. Analysis of HDG methods for Oseen equations. *J. Sci. Comput.*, 55(2):392–431, May 2013.

[9] A. Cesmelioglu, B. Cockburn, and W. Qiu. Analysis of a hybridizable discontinuous Galerkin method for the steady-state incompressible Navier–Stokes equations. *Math. Comp.*, 86(306):1643–1670, 2017.

[10] H. Chen, P. Lu, and X. Xu. A hybridizable discontinuous Galerkin method for the Helmholtz equation with high wave number. *SIAM Journal on Numerical Analysis*, 51(4):2166–2188, 2013.

[11] H. Chen, W. Qiu, and K. Shi. A priori and computable a posteriori error estimates for an HDG method for the coercive Maxwell equations. *Computer Methods in Applied Mechanics and Engineering*, 333:287 – 310, 2018.

[12] H. Chen, W. Qiu, K. Shi, and M. Solano. A superconvergent HDG method for the Maxwell equations. *Journal of Scientific Computing*, 70(3):1010–1029, 2017.

[13] Y. Chen and B. Cockburn. Analysis of variable-degree HDG methods for convection-diffusion equations. Part I: general nonconforming meshes. *IMA Journal of Numerical Analysis*, 32(4):1267–1293, Feb. 2012.

[14] Y. Chen and B. Cockburn. Analysis of variable-degree HDG methods for convection-diffusion equations. part II: Semimatching nonconforming meshes. *Mathematics of Computation*, 83(285):87–111, May 2013.

[15] B. Cockburn, J. Gopalakrishnan, and J. Guzmán. A new elasticity element made for enforcing weak stress symmetry. *Mathematics of Computation*, 79(271):1331–1349, 2010.

[16] B. Cockburn, J. Gopalakrishnan, and R. Lazarov. Unified hybridization of discontinuous Galerkin, mixed, and continuous Galerkin methods for second order elliptic problems. *SIAM J. Numer. Anal.*, 47(2):1319–1365, 2009.

[17] B. Cockburn, J. Gopalakrishnan, N. C. Nguyen, J. Peraire, and F.-J. Sayas. Analysis of HDG methods for Stokes flow. *Math. Comp.*, 80:723–760, 2011.

[18] B. Cockburn, J. Gopalakrishnan, and F.-J. Sayas. A projection-based error analysis of HDG methods. *Mathematics of Computation*, 79(271):1351–1367, Mar. 2010.

[19] B. Cockburn, W. Qiu, and M. Solano. A priori error analysis for HDG methods using extensions from subdomains to achieve boundary conformity. *Mathematics of Computation*, 83, 03 2014.

[20] B. Cockburn and K. Shi. Superconvergent HDG methods for linear elasticity with weakly symmetric stresses. *IMA Journal of Numerical Analysis*, 33(3):747–770, 10 2012.

[21] B. Cockburn and M. Solano. Solving Dirichlet boundary-value problems on curved domains by extensions from subdomains. *SIAM Journal on Scientific Computing*, 34(1):A497–A519, 2012.

[22] D. A. Di Pietro and A. Ern. *Mathematical Aspects of Discontinuous Galerkin Methods*. Springer Berlin Heidelberg, 2012.

[23] C. Domínguez, G. N. Gatica, and S. Meddahi. A posteriori error analysis of a fully-mixed finite element method for a two-dimensional fluid-solid interaction problem. *Journal of Computational Mathematics*, 33(6):606–641, 2015.

[24] B. Engquist and A. Majda. Absorbing boundary conditions for the numerical simulation of waves. *Mathematics of Computation*, 31(139):629–651, 1977.

[25] X. Feng, P. Lu, and X. Xu. A hybridizable discontinuous Galerkin method for the time-harmonic Maxwell equations with high wave number. *Computational Methods in Applied Mathematics*, 16(3):429–445, 2016.

[26] G. Fu, Y. Jin, and W. Qiu. Parameter-free superconvergent $H(\text{div})$-conforming HDG methods for the Brinkman equations. *arXiv:1607.07662 [math.NA]*, July 2016.

[27] G. Fu, W. Qiu, and W. Zhang. An analysis of HDG methods for convection–dominated diffusion problems. *ESAIM: M2AN*, 49(1):225–256, 2015.

[28] G. N. Gatica, N. Heuer, and S. Meddahi. Coupling of mixed finite element and stabilized boundary element methods for a fluid–solid interaction problem in 3d. *Numerical Methods for Partial Differential Equations*, 30(4):1211–1233, 2014.

[29] G. N. Gatica, A. Márquez, and S. Meddahi. Analysis of the coupling of Lagrange and Arnold-Falk-Winther finite elements for a fluid-solid interaction problem in three dimensions. *SIAM Journal on Numerical Analysis*, 50(3):1648–1674, 2012.

[30] G. N. Gatica and F. A. Sequeira. A priori and a posteriori error analyses of an augmented HDG method for a class of quasi-Newtonian Stokes flows. *J. Sci. Comput.*, 69:1192–1250, 2016.

[31] G. N. Gatica and F. A. Sequeira. Analysis of the HDG method for the Stokes–Darcy coupling. *Numer. Methods Partial Differential Equations*, 33(3):885–917, 2017.

[32] R. Griesmaier and P. Monk. Error analysis for a hybridizable discontinuous Galerkin method for the Helmholtz equation. *Journal of Scientific Computing*, 49(3):291–310, 2011.

[33] J. Guzmán. A unified analysis of several mixed methods for elasticity with weak stress symmetry. *Journal of Scientific Computing*, 44:156–169, 2010.

[34] L. Halpern and L. N. Trefethen. Wide-angle one-way wave equations. *The Journal of the Acoustical Society of America*, 84(4):1397–1404, 10 1988.

[35] R. L. Higdon. Numerical absorbing boundary conditions for the wave equation. *Mathematics of Computation*, 49(179):65–90, 1987.

[36] G. C. Hsiao and T. Sánchez-Vizuet. Time-dependent wave-structure interaction revisited: Thermo-piezoelectric scatterers. *Fluids*, 6(3), 2021. (arXiv: 2102.04118).

[37] G. C. Hsiao, T. Sánchez-Vizuet, and F.-J. Sayas. Boundary and coupled boundary-finite element methods for transient wave-structure interaction. *IMA Journal of Numerical Analysis*, 37(1):237–265, 2016. (arXiv:1509.01713).

[38] L. N. T. Huynh, N. C. Nguyen, J. Peraire, and B. C. Khoo. A high-order hybridizable discontinuous Galerkin method for elliptic interface problems. *International Journal for Numerical Methods in Engineering*, 93(2):183–200, jan 2013.

[39] Q.-H. Liu and J. Tao. The perfectly matched layer for acoustic waves in absorptive media. *The Journal of the Acoustical Society of America*, 102(4):2072–2082, 10 1997.

[40] J. Manríquez, N.-C. Nguyen, and M. Solano. A dissimilar non-matching HDG discretization for Stokes flows. *Comput. Methods Appl. Mech. Engrg.*, 399:Paper No. 115292, 30, 2022.

[41] S. Meddahi, D. Mora, and R. Rodríguez. Finite element analysis for a pressure–stress formulation of a fluid–structure interaction spectral problem. *Computers & Mathematics with Applications*, 68(12, Part A):1733–1750, 2014.

[42] R. Mottier, A. Ern, R. Khot, and L. Guillot. Hybrid high-order methods for elasto-acoustic wave propagation in the time domain. *ESAIM: Mathematical Modelling and Numerical Analysis*, 59(5):2685–2715, Sept. 2025.

[43] N. C. Nguyen, J. Peraire, and B. Cockburn. An implicit high–order hybridizable discontinuous Galerkin method for linear convection–diffusion equations. *J. Comput. Phys.*, 228(9):3232–3254, 2009.

[44] N. C. Nguyen, J. Peraire, and B. Cockburn. Hybridizable discontinuous Galerkin methods for the time-harmonic Maxwell's equations. *Journal of Computational Physics*, 230(19):7151–7175, 2011.

[45] N. C. Nguyen, J. Peraire, and B. Cockburn. An implicit high-order hybridizable discontinuous Galerkin method for the incompressible Navier–Stokes equations. *J. Comput. Phys.*, 230(4):1147–1170, 2011.

[46] W. Qiu, J. Shen, and K. Shi. HDG method for linear elasticity with strong symmetric stresses. *Mathematics of Computations*, 87:69–93, 2018.

[47] N. Sánchez, T. Sánchez-Vizuet, and M. Solano. Error analysis of an unfitted HDG method for a class of non-linear elliptic problems. *Journal of Scientific Computing*, 90(3), Feb. 2022. (arXiv: 2105.03560).

[48] N. Sánchez, T. Sánchez-Vizuet, and M. E. Solano. A priori and a posteriori error analysis of an unfitted HDG method for semi-linear elliptic problems. *Numerische Mathematik*, 148(4):919–958, Aug. 2021. (arXiv:1911.12298).

[49] N. Sánchez, T. Sánchez-Vizuet, and M. E. Solano. Afternote to "Coupling at a Distance": Convergence analysis and a priori error estimates. *Computational Methods in Applied Mathematics*, 22(4):945–970, 2022.

[50] T. Sánchez-Vizuet. *Integral and coupled integral-volume methods for transient problems in wave-structure interaction*. Phd thesis, University of Delaware, Newark, DE, 2016. Available at https://udspace.udel.edu/items/88d8c2c7-633a-456c-90b7-4a7a60ca7317.

[51] T. Sánchez-Vizuet. A symmetric boundary integral formulation for time-domain acoustic-elastic scattering. *Computational Mechanics*, 2025. (In press) arXiv:2502.04767.

[52] T. Sánchez-Vizuet and M. E. Solano. A Hybridizable Discontinuous Galerkin solver for the Grad-Shafranov equation. *Computer Physics Communications*, 235:120 – 132, 2019. (arXiv:1712.04148).

[53] T. Sánchez-Vizuet, M. E. Solano, and A. J. Cerfon. Adaptive hybridizable discontinuous Galerkin discretization of the Grad-Shafranov equation by extension from polygonal subdomains. *Computer Physics Communications*, 255:107239, 2020. (arXiv:1903.01724).

[54] M. Solano, S. Terrana, N.-C. Nguyen, and J. Peraire. An HDG method for dissimilar meshes. *IMA J. Numer. Anal.*, 42(2):1665–1699, 2022.

[55] L. N. Trefethen and L. Halpern. Well-posedness of one-way wave equations and absorbing boundary conditions. *Mathematics of Computation*, 47(176):421–435, 1986.

[56] B. Wang and B. C. Khoo. Hybridizable discontinuous Galerkin method (HDG) for Stokes interface flow. *Journal of Computational Physics*, 247:262–278, Aug. 2013.

[57] B. Zhu and H. Wu. Preasymptotic error analysis of the HDG method for Helmholtz equation with large wave number. *Journal of Scientific Computing*, 87(2):1–34, 2021.

Centro de Investigación en Ingeniería Matemática (CI²MA)

PRE-PUBLICACIONES 2025

2025-11 Ramiro Acevedo, Rommel Bustinza, Christian Gómez: *A transient Eddy current problem via potential formulation with current excitation*

2025-12 Abraham J. Arenas, Juan Barajas-Calonge, Gilberto González-Parra, Luis M. Villada: *A second-order nonstandard finite difference scheme for eco-epidemiological predator-prey models*

2025-13 Alonso J. Bustos, Sergio Caucao, Gabriel N. Gatica: *Mixed-primal and fully-mixed formulations for the convection-diffusion-reaction system based upon Brinkman–Forchheimer equations*

2025-14 Gabriel N. Gatica, Zeinab Gharibi, Ricardo Oyarzúa: *Banach spaces-based fully mixed finite element methods for the n-dimensional Boussinesq problem with temperature-dependent parameters*

2025-15 Sergio Caucao, Ricardo Oyarzúa, Segundo Villa-Fuentes: *A priori and a posteriori error analyses of a fully-mixed finite element method for the coupled Navier Stokes / Darcy problem*

2025-16 Juan Barajas-Calonge, Raimund Bürger, Pep Mulet, Luis M. Villada: *A second-order invariant-region-preserving scheme for a transport-flow model of polydisperse sedimentation*

2025-17 Raimund Bürger, Stefan Diehl, María Carmen Martí, Yolanda Vásquez: *A numerical scheme for a model of a flotation column including the transport of liquid components*

2025-18 Raimund Bürger, Enrique D. Fernández Nieto, José Garres-Díaz, Jorge Moya: *Well-balanced physics-based finite volume schemes for Saint-Venant-Exner-type models of sediment transport*

2025-19 Harold D. Contreras, Paola Goatin, Luis M. Villada: *Well-posedness of a nonlocal upstream-downstream traffic model*

2025-20 Thierry Coulbois, Anahi Gajardo, Pierre Guillon, Victor H. Lutfalla: *Aperiodic monotiles: from geometry to groups*

2025-21 Esteban Henriquez, Tonatiuh Sanchez-Vizuet, Manuel Solano: *An unfitted HDG discretization for a model problem in shape optimization*

2025-22 Fernando Artaza-Covarrubias, Tonatiuh Sanchez-Vizuet, Manuel Solano: *A coupled HDG discretization for the interaction between acoustic and elastic waves*

Para obtener copias de las Pre-Publicaciones, escribir o llamar a: Director, Centro de Investigación en Ingeniería Matemática, Universidad de Concepción, Casilla 160-C, Concepción, Chile, Tel.: 41-2661324, o bien, visitar la página web del centro: http://www.ci2ma.udec.cl

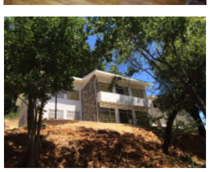

Centro de Investigación en Ingeniería Matemática (CI^{2}MA)
Universidad de Concepción

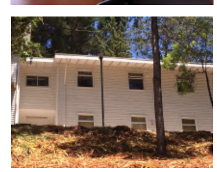

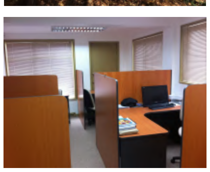

Casilla 160-C, Concepción, Chile
Tel.: 56-41-2661324/2661554/2661316
http://www.ci2ma.udec.cl